

# The role of environmental driving factors in historical and projected carbon dynamics of wetland ecosystems in Alaska

ZHOU LYU,<sup>1</sup> HÉLÈNE GENET,<sup>2</sup> YUJIE HE,<sup>1</sup> QIANLAI ZHUANG,<sup>1,10</sup> A. DAVID MCGUIRE,<sup>3</sup> ALEC BENNETT,<sup>4</sup> AMY BREEN,<sup>4</sup> JOY CLEIN,<sup>2</sup> EUGÉNIE S. EUSKIRCHEN,<sup>2</sup> KRISTOFER JOHNSON,<sup>5</sup> TOM KURKOWSKI,<sup>4</sup> NEAL J. PASTICK,<sup>6,7</sup> T. SCOTT RUPP,<sup>4</sup> BRUCE K. WYLIE,<sup>8</sup> AND ZHILIANG ZHU<sup>9</sup>

<sup>1</sup>*Earth, Atmospheric, and Planetary Sciences, Purdue University, West Lafayette, Indiana 47907 USA*

<sup>2</sup>*Institute of Arctic Biology, University of Alaska Fairbanks, Fairbanks, Alaska 99775 USA*

<sup>3</sup>*U.S. Geological Survey, Alaska Cooperative Fish and Wildlife Research Unit, University of Alaska Fairbanks, Fairbanks, Alaska 99775 USA*

<sup>4</sup>*Scenarios Network for Alaska and Arctic Planning, International Arctic Research Center, University of Alaska Fairbanks, Fairbanks, Alaska 99775 USA*

<sup>5</sup>*U.S. Department of Agriculture, Forest Service, Northern Research Station, Newtown Square, Pennsylvania 19073 USA*

<sup>6</sup>*Department of Forest Resources, University of Minnesota, St. Paul, Minnesota 55108 USA*

<sup>7</sup>*Stinger Ghaffarian Technologies Inc., contractor to the U.S. Geological Survey, Sioux Falls, South Dakota 57198 USA*

<sup>8</sup>*U.S. Geological Survey, The Earth Resources Observation Systems Center, Sioux Falls, South Dakota 57198 USA*

<sup>9</sup>*U.S. Geological Survey, Reston, Virginia 12201 USA*

**Abstract.** Wetlands are critical terrestrial ecosystems in Alaska, covering ~177,000 km<sup>2</sup>, an area greater than all the wetlands in the remainder of the United States. To assess the relative influence of changing climate, atmospheric carbon dioxide (CO<sub>2</sub>) concentration, and fire regime on carbon balance in wetland ecosystems of Alaska, a modeling framework that incorporates a fire disturbance model and two biogeochemical models was used. Spatially explicit simulations were conducted at 1-km resolution for the historical period (1950–2009) and future projection period (2010–2099). Simulations estimated that wetland ecosystems of Alaska lost 175 Tg carbon (C) in the historical period. Ecosystem C storage in 2009 was 5,556 Tg, with 89% of the C stored in soils. The estimated loss of C as CO<sub>2</sub> and biogenic methane (CH<sub>4</sub>) emissions resulted in wetlands of Alaska increasing the greenhouse gas forcing of climate warming. Simulations for the projection period were conducted for six climate change scenarios constructed from two climate models forced under three CO<sub>2</sub> emission scenarios. Ecosystem C storage averaged among climate scenarios increased 3.94 Tg C/yr by 2099, with variability among the simulations ranging from 2.02 to 4.42 Tg C/yr. These increases were driven primarily by increases in net primary production (NPP) that were greater than losses from increased decomposition and fire. The NPP increase was driven by CO<sub>2</sub> fertilization (~5% per 100 parts per million by volume increase) and by increases in air temperature (~1% per °C increase). Increases in air temperature were estimated to be the primary cause for a projected 47.7% mean increase in biogenic CH<sub>4</sub> emissions among the simulations (~15% per °C increase). Ecosystem CO<sub>2</sub> sequestration offset the increase in CH<sub>4</sub> emissions during the 21st century to decrease the greenhouse gas forcing of climate warming. However, beyond 2100, we expect that this forcing will ultimately increase as wetland ecosystems transition from being a sink to a source of atmospheric CO<sub>2</sub> because of (1) decreasing sensitivity of NPP to increasing atmospheric CO<sub>2</sub>, (2) increasing availability of soil C for decomposition as permafrost thaws, and (3) continued positive sensitivity of biogenic CH<sub>4</sub> emissions to increases in soil temperature.

**Key words:** Alaska; Alaska carbon cycle; atmospheric CO<sub>2</sub>; carbon balance; climate change; fire; global warming potential; methane; wetlands.

## INTRODUCTION

Based on records that date back to the middle of the 19th century, global mean surface temperature has risen by 0.4°C (IPCC, Climate Change, 2014). In the northern hemisphere, climatic changes have been more rapid and pronounced than in regions further south (Manabe and Stouffer 1980, Forster et al. 2000, Alexeev 2003, Alexeev et al. 2005, Cai 2006,

McGuire et al. 2006, Winton 2006, Cai and Lu 2007, Langen and Alexeev 2007, Graversen and Wang 2009). Alaska has experienced warming since the beginning of the 20th century and, since the 1970s, the temperature increase has been substantial (Hartmann and Wendler 2005, Wendler and Shulski 2009, Pastick et al. 2017). In the Arctic, warming has been 1–1.5 times faster than the global mean increase, with roughly 0.6°C rise per decade over the past 30 yr (IPCC, Climate Change, 2014). While the signatories to the United Nations Framework Convention on Climate Change aim to stabilize atmospheric greenhouse gases concentration, it is believed that the warming trend will continue into the future (IPCC, Climate Change, 2014). Simulations by general circulation models (GCMs) suggest that a

Manuscript received 11 October 2017; revised 5 April 2018; accepted 13 April 2018. Corresponding Editor: Yude Pan.

**Editor's Note:** Papers in Invited Features are published individually and will be linked online in a virtual table of contents.

<sup>10</sup>Corresponding author. E-mail: qzhuang@purdue.edu

2°C increase in global mean surface temperature relative to the preindustrial temperatures would result in a 3.2°–6.6°C increase in the Arctic by the middle of the 21st century (Kaplan and New 2006).

Despite its lower magnitude compared to carbon dioxide (CO<sub>2</sub>) fluxes, methane (CH<sub>4</sub>) dynamic is an important component of the global climate system (Fisher et al. 2014). It is the third most abundant greenhouse gas in the atmosphere, with a 100-yr global warming potential (GWP) 25 times higher than that of CO<sub>2</sub> (Forster et al. 2007). Increases in atmospheric CH<sub>4</sub> have been responsible for about 20% of the global warming caused by greenhouse gases since the preindustrial time (Dlugokencky et al. 1998). Historically, wetlands have played important roles in the global CH<sub>4</sub> budget as the single largest natural emitter. Approximately 10% of global CH<sub>4</sub> fluxes (35 Tg/yr) have been attributed to emissions from high-latitude wetlands north of 50°N (Sebacher et al. 1985, Matthews and Fung 1987, Crill et al. 1988, Fung et al. 1991, Reeburgh and Whalen 1992, Zhuang et al. 2004, McGuire et al. 2009, Thornton et al. 2016). Emissions from natural wetlands are thought to be partially responsible for the recent rise in global CH<sub>4</sub> concentration (Kirschke et al. 2013), reaching 1,820 ppb by 2012, with an increase rate of  $5.2 \pm 0.2$  ppb/yr during 2008–2012 (mean  $\pm$  SD; Saunio et al. 2017).

Wetlands in northern high latitudes account for 44% of the global wetland area (OECD 1996). Wetlands in Alaska cover roughly 12% (177,069 km<sup>2</sup>) of the total land surface area (Pastick et al. 2017), which is larger than all the wetlands in the rest of the United States (Burkett and Kusler 2000). As a transitional zone between aquatic and terrestrial ecosystems, wetlands are characterized by poorly drained soils that allow rapid accumulation of carbon (C) in thick peat layers. In regions with permafrost, this peat can also become protected from decomposition as it is incorporated into permafrost (Burkett and Kusler 2000, O'Donnell et al. 2011). The amount of C stored in the top 100 cm of northern peatlands is estimated to be  $472 \pm 27$  Pg (mean  $\pm$  SD), roughly 37% of global terrestrial C (Fao and Isric 2012, Hugelius et al. 2014). High-latitude wetlands also release C in the form of CO<sub>2</sub> and CH<sub>4</sub> in response to aerobic and anaerobic decomposition, respectively (Zhuang et al. 2004, 2007, Johnston et al. 2014, Mondav et al. 2014). With increased permafrost thaw driven by climate warming, the amount of unfrozen organic matter available for decomposition is expected to increase and result in an increase in soil CO<sub>2</sub> and CH<sub>4</sub> releases (Schuur et al. 2008, Koven et al. 2011, Schaefer et al. 2011).

As biogenic CH<sub>4</sub> emissions from anaerobic wetlands are the primary source of natural CH<sub>4</sub> emissions in North America (Kirschke et al. 2013), it is important to assess how these emissions will respond to environmental change during the remainder of this century in Alaska. CH<sub>4</sub> emissions from wetlands are controlled by many factors, including climate, atmospheric CO<sub>2</sub> concentration, and electron acceptor availability in the soil (Zehnder and Stumm 1988, Wang et al. 1993, Whiting and Chanton 1993). In particular, it is expected that CH<sub>4</sub> emissions may be very responsive to soil temperature and moisture changes resulting from climate change (Updegraff et al. 2001, Turetsky et al. 2008, Olefeldt et al. 2013, Ma et al. 2017).

Besides assessing the response of biogenic CH<sub>4</sub> emissions of wetlands in Alaska, it is also important to assess how the uptake and release of CO<sub>2</sub> will be influenced by changes in atmospheric CO<sub>2</sub>, climate, and wildfire. Changes in air and soil temperature and in hydrology have been documented to influence the exchange of CO<sub>2</sub> in wetlands in Alaska (Olefeldt et al. 2017). Although wetlands do not burn as frequently as upland ecosystems due to low flammability associated with moist soils, they do burn in very hot and dry years and can lose a significant amount of C to the atmosphere from fire emissions (Turetsky et al. 2011). Northern silty wetlands with shallow permafrost are more vulnerable to post-fire permafrost thaw and associated soil C loss than well-drained rocky uplands (Minsley et al. 2016). In recent years, extended dry periods and more frequent late-season burning, along with continued change in the permafrost and drainage conditions, have combined to increase the potential for wetlands to lose deep organic matter through burning (Kasischke and Turetsky 2006, Turetsky et al. 2011).

In this study, we assessed how C dynamics of wetland ecosystems in Alaska have changed during the historical period (1950–2009) and may change during the projection period (2010–2099) in response to changing atmospheric CO<sub>2</sub>, climate, and fire regime. Two existing process-based terrestrial ecosystem models, which were calibrated and tested for the major vegetation types in wetlands of Alaska, and a state and transition disturbance model were applied in this study. Future projections of C stocks, CO<sub>2</sub>, and CH<sub>4</sub> dynamics were simulated using six climate scenarios from two GCMs for three atmospheric CO<sub>2</sub> emission scenarios. Changes in C dynamics were analyzed for the four main Landscape Conservation Cooperative (LCC) regions of Alaska: (1) Arctic LCC, (2) Western Alaska LCC, (3) Northwest boreal LCC, and (4) North Pacific LCC (Fig. 1). With the goal of improving our understanding of the mechanisms responsible for the projections of C dynamics of wetlands in Alaska, we conducted an attribution analysis to quantify the effects of increases in atmospheric CO<sub>2</sub>, changes in climate, and changes in fire regime on wetland C accumulation and CO<sub>2</sub> and CH<sub>4</sub> dynamics.

## MATERIALS AND METHODS

### *Model framework*

Wetland C dynamics have been assessed using a model framework identical to the one described in Genet et al. (2017). C stocks and CO<sub>2</sub> fluxes were simulated using the Dynamic Organic Soil version of the Terrestrial Ecosystem Model (DOS-TEM; see Yi et al. 2009, 2010 for model structure and dynamics). DOS-TEM is a process-based biogeochemical model that estimates soil and vegetation thermal and hydrological regimes, permafrost dynamics, and carbon and nitrogen fluxes between soil, vegetation, and the atmosphere, and carbon and nitrogen pools in the soil and the vegetation (more detailed description of the model can be found in Genet et al. 2017). CH<sub>4</sub> fluxes were simulated using the Methane Dynamics Module of the Terrestrial Ecosystem Model (MDM-TEM; Zhuang et al. 2004). MDM-TEM is a process-based biogeochemical model that estimates the net flux of CH<sub>4</sub> between soils and the atmosphere based on the

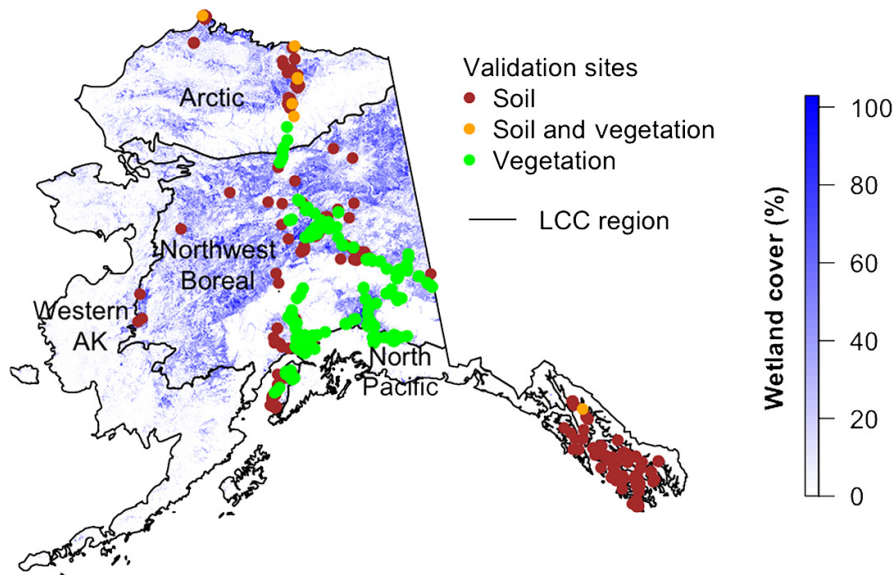


FIG. 1. Wetland distribution across Alaska (AK) and the boundaries of the four Landscape Conservation Cooperative regions of the assessment analysis. The brown, orange, and green dots represent observation sites used for model validation of the soil, the soil and the vegetation, and the vegetation carbon pools, respectively. Wetland percent cover is depicted at a 1-km resolution.

rate of  $\text{CH}_4$  production and oxidation within the soil profile, and the transport of  $\text{CH}_4$  from the soil to the atmosphere (see the detailed description of MDM-TEM in *MDM-TEM description*). Finally, projections of the fire regime in response to climate were produced by the Alaska Frame-Based Ecosystem Code (ALFRESCO; Rupp et al. 2000, 2002, 2007, Johnstone et al. 2011, Mann et al. 2012, Gustine et al. 2014). ALFRESCO is a spatially explicit, stochastic landscape succession model designed and parameterized for Arctic and sub-Arctic regions (see Pastick et al. [2017] for a detailed description of ALFRESCO and for validation of the historical fire regime simulated by ALFRESCO). The three models were coupled asynchronously, where information on fire occurrence produced by ALFRESCO was used to drive DOS-TEM and information on vegetation net primary productivity (NPP) and leaf area index (LAI) produced by DOS-TEM was used to drive MDM-TEM (Fig. 2).

#### *MDM-TEM description*

MDM-TEM is a process-based ecosystem model that simulates biogenic  $\text{CH}_4$  fluxes ( $\text{BioCH}_4$ ) in terrestrial ecosystems. MDM-TEM explicitly considers the processes of  $\text{CH}_4$  production, transport, and oxidation between the soil and atmosphere on a daily time step (Zhuang et al. 2004). MDM has been designed to be coupled to the existing TEM modeling framework that includes terrestrial carbon and nitrogen dynamics, a soil thermal module for simulating permafrost dynamics, and a hydrological module that simulates movement of water within the atmosphere–vegetation–soil continuum and water table depth (Zhuang et al. 2002, 2003, 2004). Water table depth is critical for simulating wetlands C dynamics in terms of partitioning soil decomposition products between  $\text{CO}_2$  and  $\text{CH}_4$ . Soil moisture dynamics are explicitly modeled in layers of moss, organic soil, and mineral soil (Zhuang et al. 2002, 2004).

MDM-TEM simulates the production and oxidation of  $\text{CH}_4$  between the soil column and the atmosphere as well as  $\text{CH}_4$  transport across the soil surface. The overall  $\text{CH}_4$  fluxes depend on the relative relationship among these three terms. Production and oxidation of  $\text{CH}_4$  are combined to represent the net emission/uptake of  $\text{CH}_4$  between the soil and the atmosphere. Net emission means that  $\text{CH}_4$  will be emitted to the atmosphere through diffusion when the rate of  $\text{CH}_4$  production (methanogenesis) exceeds that of oxidation (methanotrophy) within the soil column. In addition to diffusion between the soil column and the atmosphere, there are two other ways that  $\text{CH}_4$  can be transported to the atmosphere in wetlands. One is ebullition, in which bubbles form when  $\text{CH}_4$  concentration is high and the water table is above the moist soil, and move through the water column to be released to the atmosphere. The other way is plant-aided  $\text{CH}_4$  transport, which happens when  $\text{CH}_4$  moves through aerenchyma tissues of vascular plants from deep root systems to aboveground leaves to escape to the atmosphere.

The soil component in MDM-TEM contains two separate layers: the upper unsaturated zone and the lower saturated zone, defined by the water table depth.  $\text{CH}_4$  production occurs in the lower saturated zone where water creates an anaerobic environment and is affected by substrate availability, soil temperature, soil pH, and availability of electron acceptors. Substrate availability is represented using a function of NPP, which is provided by DOS-TEM (Fig. 2). A  $Q_{10}$  function is used to calculate the effects of soil temperature on  $\text{CH}_4$  production, with a reference temperature from previous calibration. Coefficients in this  $Q_{10}$  function are ecosystem specific, and each grid cell has a prescribed ecosystem type. The optimum soil pH is set to 7.5 for wetlands in Alaska. Finally, the effect of electron acceptor availability is implemented using a multiplier that relates to redox potential on  $\text{CH}_4$  production. The multiplier, which is determined by calibration, diminishes linearly if redox potential exceeds

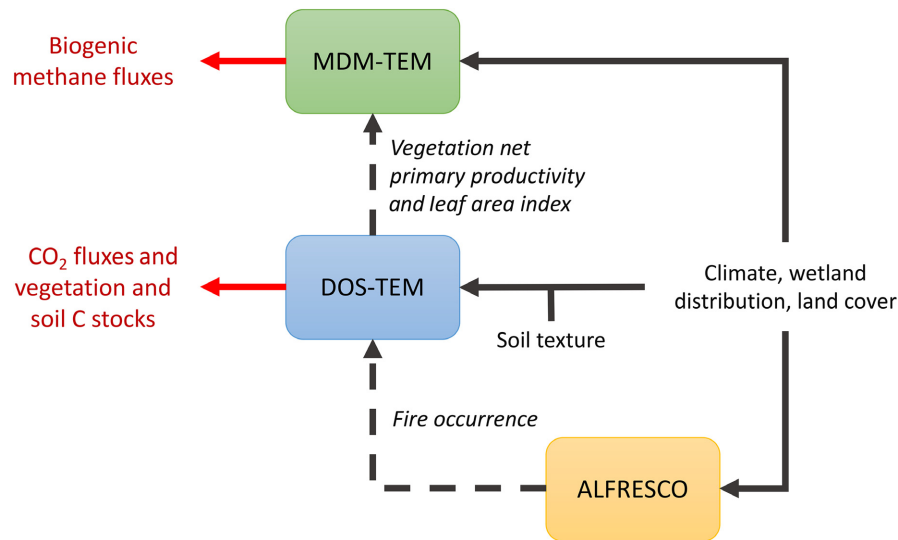


FIG. 2. Modeling framework developed for this study, coupling the Dynamic Organic Soil version of the Terrestrial Ecosystem Model (DOS-TEM, blue box), the Methane Dynamics Module of the Terrestrial Ecosystem Model (MDM-TEM, green box), and the Alaska Frame-Based Ecosystem Code (ALFRESCO, orange box). Black text and solid arrows represent input drivers. Black text and dotted arrows represent flows of information within and among models. Red text and arrows represent outputs.

–200 mV, or is set as 1.0 (Fiedler and Sommer 2000, Zhuang et al. 2002).  $\text{CH}_4$  oxidation is simulated in the unsaturated zone of the soil column when the soil moisture is within a prescribed ecosystem-specific range that allows methanotrophy (Zhuang et al. 2004).  $\text{CH}_4$  oxidation is affected by both soil moisture and temperature. A  $Q_{10}$  function is used with ecosystem-specific reference temperatures to simulate enhanced oxidation with rising soil temperature. Soil moisture influences  $\text{CH}_4$  oxidation negatively when it is not at the optimum level. Substrate availability affects  $\text{CH}_4$  oxidation following a Michaelis-Menten function. Finally, increasing redox potential from –200 to 200 mV enhances  $\text{CH}_4$  oxidation (Zhuang et al. 2002, 2004).

#### MDM-TEM parameterization and validation

MDM-TEM is parameterized for three typical types of wetland ecosystems in Alaska based on specific plant types and hydrological characteristics (Table 1). The land cover map used for the simulations in this study defined seven wetland cover types in Alaska, which were grouped into the three wetland types parameterized in MDM-TEM as follows: (1) lowland black spruce (*Picea mariana* (Mill.) Britton, Sterns & Poggenb.), white spruce (*Picea glauca* (Moench) Voss), deciduous forests, and maritime wetland forest were classified as boreal wetland in MDM-TEM; (2) graminoid tundra was classified as mesic wetland tundra; and (3) wet sedge tundra and maritime fen were classified as wet wetland tundra.  $\text{CH}_4$  flux measurements and key soil and climate factors from three wetland field sites in Alaska tundra wetlands and Canadian wetlands north of 53° N (first three sites in Table 1) were used to parameterize MDM-TEM. These sites were representative of the mesic and wet wetland tundra and boreal wetland present in Alaska. The model was parameterized by minimizing the differences between the observed and simulated  $\text{CH}_4$  fluxes at Toolik-D, Toolik-W (Arctic LCC, Alaska), and SSA-

FEN (Saskatchewan, Canada) field sites, respectively. Initial parameter values for each of the three sites were determined from literature review. The range was set for each individual parameter in the three sets of parameters based on literature review, and adjustments were made to each parameter to minimize the root mean square error (RMSE) between the daily simulated and observed  $\text{CH}_4$  fluxes. The adjustment was conducted sequentially for all parameters until the minimized RMSE was 665, 1,729, and 1,396  $\text{mg CO}_2\text{-eq}\cdot\text{m}^{-2}\cdot\text{d}^{-1}$ , for Toolik-D, Toolik-W, and SSA-FEN sites, respectively (He et al. 2016).

To test the performance and validate parameterizations of MDM-TEM, we conducted simulations using data independent of the data we used for parameterization and calibration. A boreal forest wetland site (NSA-FEN) in Canada was used to validate the parameterization from the SSA-FEN site (Table 1). Monthly mean simulated  $\text{CH}_4$  fluxes were compared to the observed net emission at the site, and the geometric mean regression between observed and simulated fluxes was significant ( $P < 0.01$ ) with an RSME of 0.9 (He et al. 2016). When applied across Alaska, MDM-TEM indicates methane emissions are from April to November for most grid cells in Alaska, and are able to capture some of the zero-curtain emissions for the North Slope of Alaska reported by Zona et al. (2016).

#### DOS-TEM parameterization and validation

Parameterization and validation of DOS-TEM were conducted using vegetation and soil carbon and nitrogen pools and fluxes; details on the DOS-TEM parameterization and validation can be found in Genet et al. (2016) and Genet et al. (2017). The sites used for DOS-TEM historical carbon pools validation are depicted in Fig. 1. DOS-TEM estimates of soil C stocks and permafrost distribution and depth were compared with recent soil carbon and permafrost data products for Alaska (Marchenko et al. 2008, Ping et al. 2008,

TABLE 1. Description of sites used for model parameterization and validation.

Site name	Location	Elevation (m)	Land cover	Wetland type in MDM-TEM	Observed data	Source and references
Tundra at Toolik Field Station (Toolik-D)	149°36' W; 68°38' N	760.0	Tussock tundra	Mesic wetland tundra	Soil temperatures at depths of 10, 20, and 50 cm, methane fluxes from 1992 and 1993	<a href="http://ecosystems.mbl.edu/ARC">http://ecosystems.mbl.edu/ARC</a> ; <a href="http://www.wrcc.dri.edu">http://www.wrcc.dri.edu</a>
Tundra at Toolik Field Station (Toolik-W)	149°36' W; 68°38' N	760.0	Wet tussock tundra	Wet wetland tundra	Soil temperatures at depths of 3, 5, 7, 9, and 11 cm, methane fluxes from 1994 and 1995	King et al. (1998)
Fen at southern study area of BOREAS (SSA-FEN)	105°57' W; 53°57' N	524.7	Complex fen with buckbean, sedges, birch, and willow	Boreal wetland	Soil temperatures at depths of 10 and 20 cm, daily evapotranspiration and eddy covariance measurements of methane fluxes for May to October of 1994 and 1995	Sellers et al. (1997), Newcomer et al. (2000), Suyker et al. (1996, 1997)
Fen at northern study area of BOREAS (NSA-FEN; validation site)	98°25' W; 55°55' N	218.0	Fen complex, including sedge, moss, moat, and shrubs	Boreal wetland	Soil temperatures at depths of 5, 10, 20, 50, and 100 cm; water table depth (1994) and chamber measurements of methane fluxes of May through September 1994 and June through October 1996	Sellers et al. (1997), Newcomer et al. (2000), Suyker et al. (1996, 1997)

Note: MDM-TEM, Methane Dynamics Module of the Terrestrial Ecosystem Model.

Johnson et al. 2011, Mishra and Riley 2012, Hugelius et al. 2014, Pastick et al. 2015, Wylie et al. 2016). These comparisons revealed the estimates of permafrost distribution and depth as well as soil C stocks simulated by DOS-TEM were well within the range of the estimates provided by the other products for wetland and adjacent lowland ecosystems (Wylie et al. 2016, Pastick et al. 2017).

#### Input data

ALFRESCO, DOS-TEM, and MDM-TEM simulations were spatially explicit. Models were run at 1-km spatial resolution using gridded forcing data from 1950 to 2099 over the state of Alaska. Annual atmospheric CO<sub>2</sub> concentration, spatially explicit monthly mean surface air temperature, total precipitation, net incoming shortwave radiation, and vapor pressure, along with spatially explicit data for wetland distribution (Pastick et al. 2017), land cover, and soil texture (Global Soil Data Task Group 2000) were used to drive the coupled models. In addition, estimates of spatially explicit monthly NPP and LAI from DOS-TEM were used by MDM-TEM to simulate CH<sub>4</sub> fluxes.

Based on the Alaska National Wetlands Inventory, a wetland distribution map was developed for this assessment to identify seasonally or year-round waterlogged ecosystems in this study (data *available online*).<sup>11</sup> This wetland map is described in Pastick et al. (2017). Wetlands typically have poor drainage and a thick organic horizon (Burkett and Kusler 2000, O'Donnell et al. 2011). Simulation results were analyzed for the four LCCs mentioned in *Introduction* (Fig. 1). Arctic LCC wetlands are 84.7% graminoid tundra and 15.3% wet sedge tundra, and the Western Alaska LCC wetlands are 27.6% graminoid tundra and 72.4% wet sedge tundra. Wetlands in the Northwest Boreal LCC are 97% percent lowland forested permafrost plateau forest (46% conifer forest and 51% deciduous forest) and 3% open wetlands (i.e., bogs and fens). Wetlands in the North Pacific LCC are 86% maritime fen and 14% maritime wetland forest (dominated by Sitka spruce [*Picea sitchensis* (Bong.) Carrière] and black cottonwood [*Populus trichocarpa* Torr. & A. Gray ex Hook.]).

Monthly climate data were linearly interpolated to a daily time step to meet the temporal resolution of MDM-TEM. Historical climate data were from the Climatic Research Unit (CRU TS 3.1; Harris et al. 2014). Future projections (2010–2099) were driven by three different fossil CO<sub>2</sub> emission trajectories for low, medium, and high ranges of emissions (B1, A1b, and A2, respectively) and climate projections from two GCMs. The two GCMs used were version 3.1-T47 of the Coupled Global Climate Model (CGCM3.1; McFarlane et al. 1992) developed by the Canadian Centre for Climate Modeling and Analysis and version 5 of the European Centre Hamburg Model (MPI-ECHAM5; Roeckner et al. 2004) developed by the Max Planck Institute (models *available online*).<sup>12,13</sup> These climate and atmospheric CO<sub>2</sub> scenarios were obtained from the World Climate Research Programme's (WCRP's) Coupled Model

<sup>11</sup> <http://www.fws.gov/wetlands/Data/State-Downloads.html>

<sup>12</sup> [www.cccma.ec.gc.ca/data/cgcm3/](http://www.cccma.ec.gc.ca/data/cgcm3/)

<sup>13</sup> [www.mpimet.mpg.de/en/wissenschaft/modelle/echam/](http://www.mpimet.mpg.de/en/wissenschaft/modelle/echam/)

TABLE 2. Summary of the environmental drivers used by the model simulations for the historical period and the six climate scenarios.

Period and scenario	MAT (°C)	SAP (mm)	Atm. CO <sub>2</sub> (ppm)	AOB (km <sup>2</sup> /yr)	VWC (m <sup>3</sup> /m <sup>3</sup> )
1950–2009					
Historical	−3.61 (0.66)	926 (33)	341 (25)	2734 (1502)	0.643 (0.022)
2010–2099					
CGCM 3.1-B1	−2.65 (0.99)	999 (70)	429 (85)	2718 (1069)	0.693 (0.015)
ECHAM5-B1	−2.51 (1.42)	978 (79)	429 (85)	3643 (1960)	0.683 (0.03)
CGCM 3.1-A1b	−2.12 (1.55)	1019 (91)	466 (132)	2832 (1226)	0.701 (0.02)
ECHAM5-A1b	−1.85 (2.19)	1007 (99)	466 (132)	4069 (1784)	0.68 (0.025)
CGCM 3.1-A2	−2.03 (1.77)	1033 (109)	482 (159)	3379 (1864)	0.702 (0.024)
ECHAM5-A2	−1.96 (2.15)	1007 (101)	482 (159)	3917 (2215)	0.66 (0.024)

Notes: The numbers in parenthesis indicate standard deviation computed on the annual data averaged across Alaska. MAT, mean annual temperature; SAP, sum of annual precipitation; Atm. CO<sub>2</sub>, annual atmospheric CO<sub>2</sub> concentration; AOB, annual area burned; VWC, volumetric water content.

Intercomparison Project phase 3 (CMIP3) multi-model data set (Meehl et al. 2007), and are aligned with the Intergovernmental Panel on Climate Change's Special Report on Emission Scenarios (IPCC-SRES; Nakicenovic et al. 2000; data set *available online*).<sup>14</sup> In addition, the effects of fire disturbance on C dynamics were evaluated using a gridded fire occurrence data set that combined (1) historical records from 1950 to 2009 from the Alaska Interagency Coordination Center large fire database (Kasischke et al. 2002) and (2) projected scenarios from ALFRESCO for future projections. Emission scenario A2 projected the largest increase in atmospheric CO<sub>2</sub> in the projection period, followed by A1b and B1 (Table 2; database available online).<sup>15</sup> Climate simulations of the ECHAM5 models were warmer and wetter than those of the CGCM 3.1. Mean annual area burned was also larger under the ECHAM5 climate simulations than under CGCM 3.1 climate simulations (Table 2). More details on the atmospheric CO<sub>2</sub>, climate and fire forcing data sets can be found in Genet et al. (2017) and Pastick et al. (2017).

#### Model application

Before conducting the transient simulations, a typical spin-up procedure was conducted for each spatial location, in which the model was driven by averaged modern forcings for that location, repeated continuously until dynamic equilibrium was achieved (i.e., constant pools and fluxes at that location). The resulting modeled ecosystem state for each spatial location then served as the starting point for the transient simulation during the historical and future periods. Gridded output was expressed per square meter and multiplied by grid cell area and the wetland percent cover per grid cell to yield total fluxes and storages. Regional estimates were obtained by summing up the grid cell estimates across each LCC region.

Estimates of vegetation C storage were derived from the sum of aboveground and belowground living biomass. Soil C stocks were composed of C stored in dead woody debris, moss, litter, the organic horizon, and the mineral horizon to depth of 1 m below the organic horizon. Historical changes in soil and vegetation C pools were evaluated as cumulative

changes from the estimate of the respective C pool at the end of 1949. Projected changes in soil and vegetation C pools were evaluated as cumulative changes from the estimate of the respective C pool at the end of 2009.

Net ecosystem carbon balance (NECB) is the difference between total C inputs and total C outputs of the ecosystem (Chapin et al. 2006). In this study, the C exchange between terrestrial and aquatic ecosystems was not estimated. Therefore, we calculated NECB as the NPP minus the combination of C losses from heterotrophic respiration (HR), fire emissions (as CO and CO<sub>2</sub>, i.e., Pyro(CO + CO<sub>2</sub>), and CH<sub>4</sub>, i.e., PyroCH<sub>4</sub>), and biogenic CH<sub>4</sub> emissions (BioCH<sub>4</sub>).

GWP was estimated taking into consideration that CH<sub>4</sub> has a larger GWP than CO<sub>2</sub>. We assumed that CH<sub>4</sub> GWP was 25 times larger than CO<sub>2</sub> GWP as estimated over a 100-yr timeframe for the 2007 IPCC Special Report on Emissions Scenarios (Forster et al. 2007). GWP values were reported in CO<sub>2</sub> equivalents after converting all C fluxes using molecular weights of CH<sub>4</sub> and CO<sub>2</sub>. Pyrogenic CH<sub>4</sub> (PyroCH<sub>4</sub>) production from wildfire was considered in addition to biogenic CH<sub>4</sub> emissions by applying emission factors among CO<sub>2</sub>, CH<sub>4</sub>, and CO on DOS-TEM simulations of French et al. (2002). The C in CO emissions was assumed to be converted to CO<sub>2</sub> in the atmosphere within 1 yr (Weinstock 1969) and added to the pyrogenic CO<sub>2</sub> emissions (Pyro(CO<sub>2</sub> + CO)). Based on these considerations, GWP was calculated as

$$\text{GWP} = -44/12 \times (\text{NPP} - \text{HR} - \text{Pyro}(\text{CO}_2 + \text{CO})) + 25 \times 16/12 \times (\text{PyroCH}_4 + \text{BioCH}_4) \quad (1)$$

A positive GWP indicates a net CO<sub>2</sub> loss from the ecosystem promoting atmospheric warming, while a negative GWP indicates a net CO<sub>2</sub> gain by the ecosystem promoting atmospheric cooling.

#### Attribution analysis

The relative effects of changes in atmospheric CO<sub>2</sub>, climate change and fire regime on ecosystem C balance were analyzed for the projection period 2010–2099. This analysis was based on model simulations that included combinations of time series with constant atmospheric CO<sub>2</sub>, detrended

<sup>14</sup> [http://www-pcmdi.llnl.gov/ipcc/about\\_ipcc.php](http://www-pcmdi.llnl.gov/ipcc/about_ipcc.php)

<sup>15</sup> <http://fire.ak.blm.gov/>

climate, and normalized fire regime. For more detail about the forcing data used for the attribution analysis, see Genet et al. (2017).

We conducted 10 coupled model simulations over Alaska wetlands in addition to the original six projection scenarios described above and hereafter referred to as CO<sub>2</sub> + climate + fire simulations: (1) a baseline simulation with constant atmospheric CO<sub>2</sub>, detrended climate and constant fire regime, hereafter baseline; (2) three simulations with increasing atmospheric CO<sub>2</sub> from the B1, A1b, and A2 emission scenarios, detrended climate, and constant fire regime, hereafter CO<sub>2</sub>; and (3) six simulations with increasing atmospheric CO<sub>2</sub> and changing climate simulations from the CGCM3.1 and ECHAM5 models, hereafter CO<sub>2</sub> + climate.

We evaluated (1) the effects of rising atmospheric CO<sub>2</sub> by comparing C dynamics between the CO<sub>2</sub> and the baseline simulations; (2) the effects of changing climate by comparing CO<sub>2</sub> + climate and CO<sub>2</sub> simulations; and (3) the effects of changing fire regime by comparing the CO<sub>2</sub> + climate + fire simulations with the CO<sub>2</sub> + climate simulations.

The effect of CO<sub>2</sub> fertilization on NPP, HR, and BioCH<sub>4</sub> was evaluated by examining the relationship between the relative change in fluxes and the change in atmospheric CO<sub>2</sub> concentration. The effect of climate change on NPP, HR, and BioCH<sub>4</sub> was evaluated by examining the relationship between the relative change in the respective C fluxes and the changes in annual mean air temperature, annual sum of

precipitation, annual mean net incoming radiation, and annual mean vapor pressure. The effect of fire regime was evaluated by examining the relationships between the relative change in area burned and the relative changes in NPP, HR, and BioCH<sub>4</sub> as well as between the relative change in area burned and the absolute change in fire emissions.

The relationships between changes in C fluxes and changes in environmental drivers were evaluated using ordinary least square regression. The differences between LCC regions were evaluated using analysis of variance. All analyses were performed using the SAS statistical package (SAS 9.4, SAS Institute, Cary, North Carolina, USA). The assumptions of normality and homoscedasticity were verified by examining residual plots. Effects were considered significant at  $P \leq 0.05$ . Averages of C stocks and fluxes are accompanied with the estimated standard deviation from annual variations (SD).

## RESULTS

### *Historical C dynamics of wetland ecosystems in Alaska from 1950 to 2009*

Across the 177,069 km<sup>2</sup> of wetland ecosystems in Alaska, as defined by Pastick et al. (2017), total C storage was estimated to be 5.56 Pg C in 2009, with about 89% stored in the soil and the rest in the vegetation (Table 3, Fig. 3a). During

TABLE 3. Mean annual change in vegetation, soil, and total C stocks for the historical period (1950–2009) and vegetation, soil, and total C stocks at the end of 2009 and in each landscape conservation cooperative (LCC) region and statewide.

Variables	Units	Arctic	Northwest boreal	North Pacific	Western Alaska	Statewide
Wetland area	km <sup>2</sup>	29,818	130,704	1,965	14,582	177,069
Vegetation C annual change	Tg C/yr	0.12	−1.13	0	0.03	−0.98
Vegetation C pool in 2009	Tg C	45.38	491.1	19.56	56.93	612.97
Soil C annual change	Tg C/yr	0.35	−2.36	0.06	0.02	−1.93
Soil C pool in 2009	Tg C	1274.78	2773.23	107.33	787.53	4,942.87
Total C annual change	Tg C/yr	0.47	−3.49	0.07	0.05	−2.91
Total C pool in 2009	Tg C	1320.16	3264.33	126.89	844.46	5,555.84

Note: Wetland area for LCC regions was estimated from the wetland map described in Pastick et al. (2017).

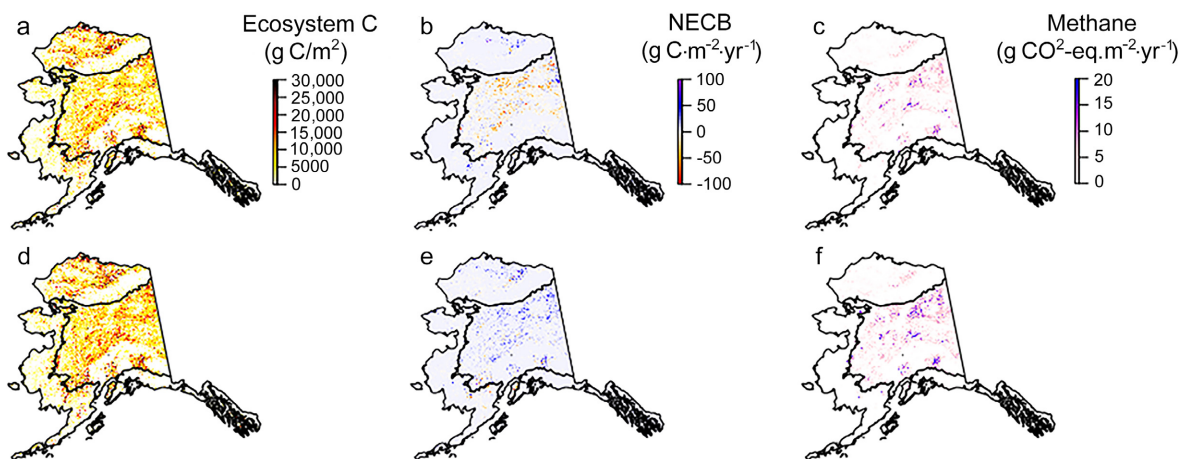


FIG. 3. Spatial distribution of wetland (a, d) ecosystem carbon stocks, (b, e) net ecosystem carbon balance, and (c, f) methane emissions for Alaska for (a–c) the historical period and (d–f) the projected period (averaged across the six climate scenarios evaluated).

the historical period, wetland ecosystems lost C from the vegetation and the soil at a rate of 2.91 Tg C/yr statewide (Fig. 3b). The accumulation of C in the Arctic, the Western Alaska, and the North Pacific LCCs was more than offset by the C loss from the Northwest Boreal LCC, the largest of the four LCC regions. C loss in the Northwest Boreal LCC occurred because the combination of HR, fire emissions, and CH<sub>4</sub> emissions was greater than NPP (Table 4).

Statewide, biogenic CH<sub>4</sub> emissions from wetlands were estimated to be 0.91 Tg C/yr during the historical period (Table 4, Fig. 3c). Biogenic CH<sub>4</sub> emissions from boreal wetlands (mean annual biogenic CH<sub>4</sub> emission of 0.868 Tg C/yr) were substantially greater than that from wetland tundra (0.018 Tg C/yr) and mesic wetland tundra (0.024 Tg C/yr; Fig. 4). The strong biogenic CH<sub>4</sub> emissions from the boreal wetlands are associated with a greater area and generally warmer soils and longer growing seasons than for other wetland types in Alaska. Our simulations

indicated that biogenic CH<sub>4</sub> emissions increased from 1950 to 2009 in all wetland types examined, although there was large interannual variability (Fig. 4). In comparison, pyrogenic CH<sub>4</sub> emissions represented only 1.7% of the total CH<sub>4</sub> emissions. Although CH<sub>4</sub> emissions were only 2.5% of NPP statewide, they dominated the positive GWP calculation with respect to the contribution of C lost as CO<sub>2</sub> during the historical period. Wetlands contributed to atmospheric warming in three out of the four LCC regions during the historical period (Table 4), resulting in a statewide GWP of 37.16 Tg CO<sub>2</sub>-eq/yr.

*Projected C dynamics of wetland ecosystems in Alaska  
from 2010 to 2099*

In contrast to the historical period, wetlands in Alaska accumulated C during the projection period. By 2099, vegetation and soil C stocks increased from the end of the

TABLE 4. Mean C fluxes into and out of Alaska wetland ecosystems for the historical period (1950–2009) in each LCC region and statewide.

Variable	Unit	Arctic	Northwest boreal	North Pacific	Western Alaska	Statewide
NPP	Tg C/yr	4.03 (0.49)	28.81 (1.44)	0.53 (0.04)	2.95 (0.18)	36.32 (2.74)
HR	Tg C/yr	-3.27 (1.22)	-27.13 (4.84)	-0.46 (0.08)	-2.49 (0.98)	-33.35 (9.37)
BioCH <sub>4</sub>	Tg C/yr	-0.075 (0.15)	-0.79 (1.83)	≪-0.01	-0.04 (0.12)	-0.91 (0.78)
PyroCH <sub>4</sub>	Tg C/yr	≪-0.01	-0.01 (0.03)	≪-0.01	≪-0.01	-0.02 (0.03)
Pyro(CO + CO <sub>2</sub> )	Tg C/yr	-0.22 (0.40)	-4.36 (7.58)	≪-0.01	-0.37 (0.69)	-4.96 (8.98)
NECB	Tg C/yr	0.47 (1.15)	-3.49 (10.46)	0.07 (0.08)	0.05 (1.06)	-2.91 (10.56)
GWP	Tg CO <sub>2</sub> -eq/yr	0.53 (1.31)	36.67 (109.90)	0.11 (0.13)	-0.15 (3.22)	37.16 (134.85)

Notes: Numbers in parenthesis indicate inter-annual standard deviation. Except for global warming potential (GWP), positive numbers indicate uptake of C into wetland ecosystems and negative numbers indicates losses of C. For GWP, positive numbers indicate C source and negative numbers indicates C sink. NA indicates not applicable. NPP, net primary production; HR, heterotrophic respiration; BioCH<sub>4</sub>, biogenic CH<sub>4</sub>; PyroCH<sub>4</sub>, pyrogenic CH<sub>4</sub>; NECB, net ecosystem carbon balance.

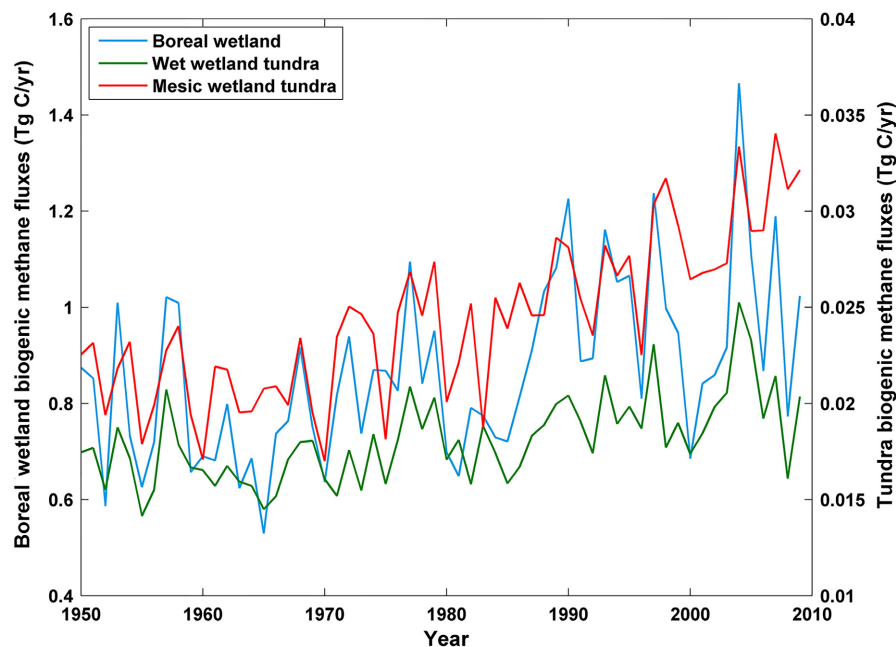


FIG. 4. Annual total methane emissions from three wetland types in Alaska during the historical period (1950–2009). Note that the units for boreal wetland fluxes are on the left y-axis and that units for the tundra wetland fluxes are on the right y-axis.

historical period in all LCC regions and for all the scenarios. Total mean C storage across the six climate scenarios was  $5,911 \pm 79.41$  Tg C (mean  $\pm$  SD; Figs. 3d, 5a), with a mean annual increase of  $3.34 \pm 0.89$  Tg C/yr (Figs. 3e, 5b) from 2010 to 2099 (Appendix S1). During that period, the largest relative increase in C storage occurred in the North Pacific LCC ( $11.4\% \pm 5.5\%$ ). The relative increase in C stocks was substantially less in the Arctic LCC ( $7.3\% \pm 1.9\%$ ), the Northwest Boreal LCC ( $6.4\% \pm 2.2\%$ ), and the Western Alaska LCC ( $4.17\% \pm 3.14\%$ ). Increases in NPP were more than offset increases in HR, fire emissions, and biogenic CH<sub>4</sub> emissions resulting in a net C sequestration statewide in all LCCs for the projection period (Fig. 5c,d; Appendix S2). Compared to the simulations for CGCM3.1 climate projections, the warmer climate projections from ECHAM5 resulted in generally greater NPP ( $8.11\%$  higher,  $F_{1/28} = 122.99$ ,  $n = 30$ ,  $P < 0.001$ ) and greater HR ( $11.38\%$  higher,  $F_{1/28} = 13.69$ ,  $n = 30$ ,  $P = 0.001$ ).

Compared to the historical period, statewide biogenic CH<sub>4</sub> increased by  $47.7\%$  on average across the projections (Fig. 3f; Appendix S2). Similar to NPP and HR, the warmer climate projections from ECHAM5 than from CGCM3.1 resulted in greater biogenic CH<sub>4</sub> emissions ( $4.16\%$  higher,  $F = 5.26$ ,  $n = 30$  and  $P = 0.031$ ). The GWP associated with the increase in CH<sub>4</sub> emissions was greater than that associated with CO<sub>2</sub> sequestration by wetland ecosystems of Alaska, resulting in a positive GWP by 2099 of  $28.37$  Tg CO<sub>2</sub>-eq/yr. Yet, compared to 2009, the positive GWP decreased by  $23.71\%$  in magnitude.

#### *Effect of environmental drivers on ecosystem C sequestration, CH<sub>4</sub> emissions, and GWP*

Changes in atmospheric CO<sub>2</sub>, climate, and wildfire each substantially affected projections of C dynamics for wetlands in Alaska. Compared to the baseline simulations, the cumulative effect of increasing atmospheric CO<sub>2</sub>, climate change, and change in fire regime resulted in a statewide increase of  $70$  Tg C in vegetation and  $240$  Tg C in soil by the end of the 21st century (i.e.,  $4.9\%$  and  $11.4\%$  increase compared to the baseline, respectively). The increase in atmospheric CO<sub>2</sub> during the projected period increased vegetation ( $70$  Tg C,  $11.4\%$ ) and soil ( $270$  Tg C,  $5.5\%$ ) C stocks substantially (Fig. 6a,b). Changes in climate increased vegetation ( $16$  Tg C,  $2.6\%$ ) and soil ( $230$  Tg C,  $4.7\%$ ) C stocks to a lesser extent. In contrast, wildfire induced a C loss in the vegetation ( $-20$  Tg C,  $-3.3\%$ ) and soil ( $-260$  Tg C,  $-5.3\%$ ) C stocks.

Compared to the baseline simulation, biogenic CH<sub>4</sub> emissions increased  $0.62$  Tg C/yr ( $68.1\%$ ) in response to the combination of changes in atmospheric CO<sub>2</sub>, climate, and wildfire by the end of the 21st century. Changes in climate substantially increased biogenic CH<sub>4</sub> emissions ( $0.91$  Tg C/yr,  $102.4\%$ ), and changes in atmospheric CO<sub>2</sub> had little effect (Fig. 6c). In contrast, changes in the fire regime decreased biogenic CH<sub>4</sub> emission by  $-0.32$  Tg C/yr ( $-35.2\%$ ).

In comparison with the baseline simulation, by the end of the 21st century, the combined effects of changes in

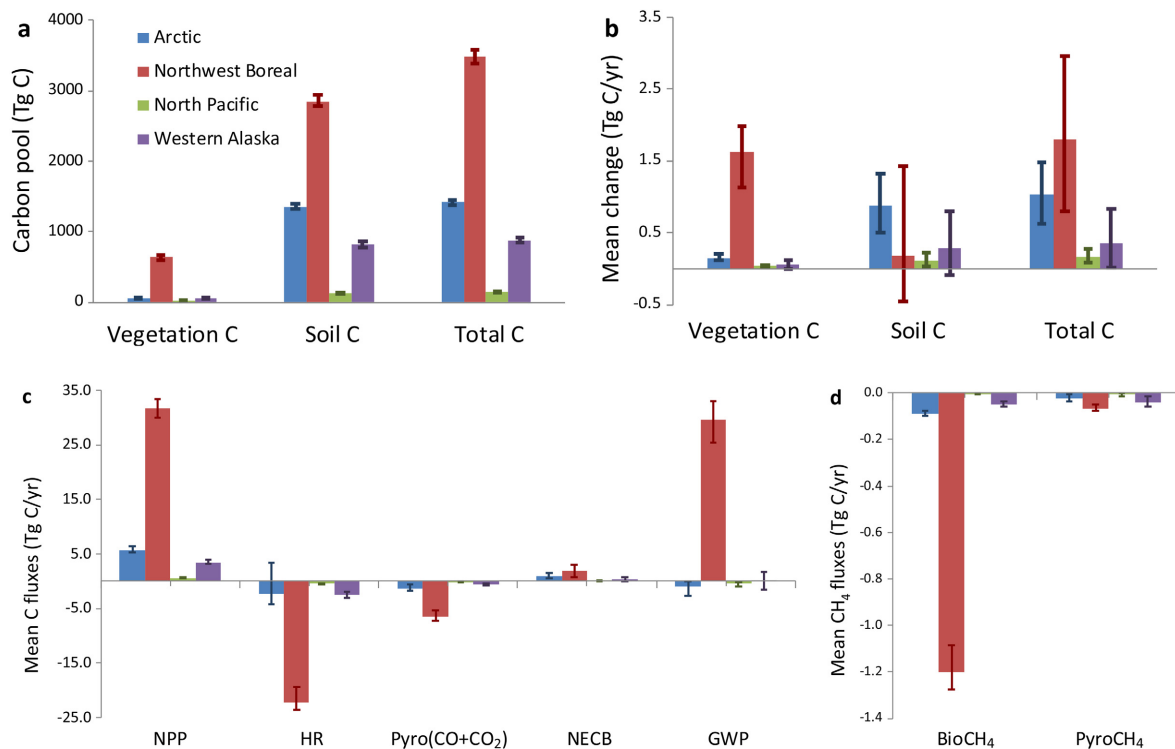


FIG. 5. (a) 2099 carbon pools, (b) 2010–2099 mean annual change in vegetation, soil, and total carbon stocks, (c) 2010–2099 mean annual CO<sub>2</sub>, and (d) CH<sub>4</sub> ecosystem fluxes, for each Landscape Conservation Cooperative region. Means are computed across the six climate scenarios. Error bars indicate the range of projections among the climate scenarios. Global Warming Potential (GWP) is depicted in panel c with the units Tg CO<sub>2</sub> equivalent/yr. Climate scenarios are described in Table 2.

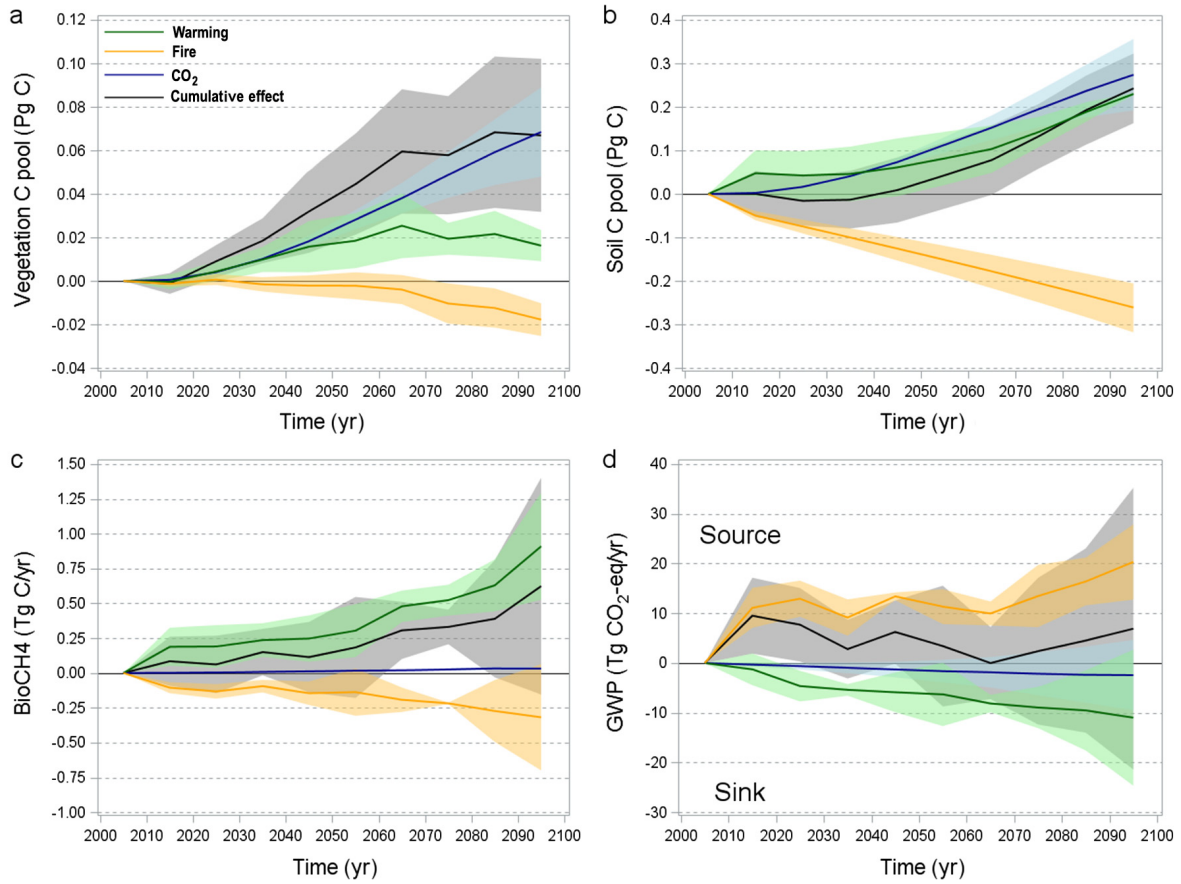


FIG. 6. Anomaly from the baseline simulation (constant atmospheric  $\text{CO}_2$ , climate, and fire regime) quantifying the cumulative effects of increasing atmospheric  $\text{CO}_2$  (blue lines), change in climate (green line) and change in fire regime (orange line) on (a) total vegetation carbon stocks, (b) total soil carbon stocks, (c) biogenic methane emissions, and (d) global warming potential across Alaska from 2010 through 2099. The black line represents the cumulative effect of increases in atmospheric  $\text{CO}_2$ , changes in climate and changes in the fire regime. The thick solid lines represent the mean among scenarios and the shaded envelopes represent the SD.

atmospheric  $\text{CO}_2$ , climate, and wildfire enhanced warming of the atmosphere by 6.91 Tg  $\text{CO}_2$ -eq/yr (18.6%) as indexed by changes in GWP (Fig. 6d). Changes in wildfire substantially enhanced climate warming (20.33 Tg  $\text{CO}_2$ -eq, 54.7%), while changes in atmospheric  $\text{CO}_2$  and climate promoted climate cooling by  $(-2.43 \text{ Tg } \text{CO}_2$ -eq/yr and  $-10.98 \text{ Tg } \text{CO}_2$ -eq/yr, respectively,  $-6.5\%$  and  $-29.6\%$ , respectively). This increase in GWP between the baseline and the simulations combining changes in atmospheric  $\text{CO}_2$ , climate, and wildfire contrasted with the decrease in GWP observed between the historical and the projection periods ( $-8.78 \text{ Tg } \text{CO}_2$ -eq/yr,  $-23.6\%$ ).

#### Biogeochemical processes affected by increasing atmospheric $\text{CO}_2$

NPP, HR, and biogenic  $\text{CH}_4$  emissions all significantly increased with increasing atmospheric  $\text{CO}_2$  (Table 5, Fig. 7). Yet, the rate of change was much lower for biogenic  $\text{CH}_4$  emissions ( $1.46\% \pm 0.09\%$  per 100 ppm increase [mean  $\pm$  SE]) than for NPP and HR ( $5.16\% \pm 0.21\%$  and  $4.66\% \pm 0.42\%$  per 100 ppm increase, respectively). All relationships between C fluxes and atmospheric  $\text{CO}_2$  concentration were significantly different among LCC regions (Table 5); the slope of the relationship between change in C fluxes and

change in atmospheric  $\text{CO}_2$  was significantly higher for the Arctic and the North Pacific LCCs than for the Northwest Boreal and the Western Alaska LCCs (Fig. 7).

#### Biogeochemical processes affected by changing climate

Because our modeling framework kept land cover static throughout the simulations, it is important to recognize that

TABLE 5. Effects of LCC region, changes in atmospheric  $\text{CO}_2$  ( $d\text{CO}_2$ ), and their interaction on projection period [2010–2099] relative changes in net primary productivity ( $d\text{NPP}$ ), heterotrophic respiration ( $d\text{HR}$ ), and biogenic methane ( $d\text{BioCH}_4$ ).

Variable	Effect	$n$	MS	$F$	$P$ -value
$d\text{NPP}$	$d\text{CO}_2$	1	519.31	$F_{1/29} = 1642.72$	<0.001
	LCC	4	13.69	$F_{4/26} = 36.83$	<0.001
	$d\text{CO}_2 * \text{LCC}$	3	4.27	$F_{3/27} = 20.58$	<0.001
$d\text{HR}$	$d\text{CO}_2$	1	537.01	$F_{1/29} = 405.88$	<0.001
	LCC	4	14.01	$F_{4/26} = 8.81$	<0.001
	$d\text{CO}_2 * \text{LCC}$	3	7.78	$F_{3/27} = 7.23$	0.004
$d\text{BioCH}_4$	$d\text{CO}_2$	1	70.16	$F_{1/29} = 1113.27$	<0.001
	LCC	4	0.46	$F_{4/26} = 7.33$	0.002
	$d\text{CO}_2 * \text{LCC}$	3	0.46	$F_{3/27} = 7.34$	0.003

Notes: MS, mean square of  $F$  test;  $F$ , Fisher value;  $P$ -value, probability.

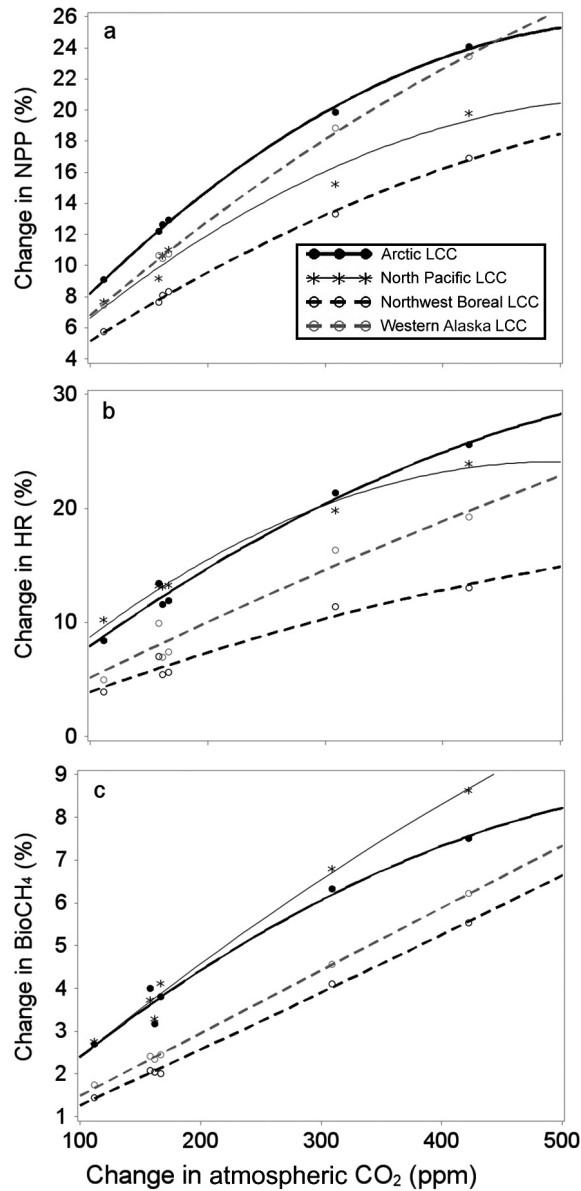


FIG. 7. Relationship between relative change in (a) net primary production (NPP), (b) heterotrophic respiration (HR), and (c) biogenic  $\text{CH}_4$  ( $\text{BioCH}_4$ ) and atmospheric  $\text{CO}_2$  from the baseline (simulations with constant atmospheric  $\text{CO}_2$ ). Different symbols and lines are depicted for each different landscape conservation cooperative (LCC) region. Each point represents the difference of decadal averages between the baseline and each atmospheric  $\text{CO}_2$  scenario. The lines represent the quadratic relationships for each LCC.

our analysis of biogeochemical processes affected by changing climate does not include the effects of changes in wetland area in response to climate change. Among the climate variables we considered in this analysis (i.e., air temperature, precipitation, vapor pressure, net incoming shortwave radiation), including modeled soil moisture of the organic horizon (Table 2), only air temperature and soil moisture changes had a significant effect on change in C fluxes. Climate warming caused a significant increase in NPP, HR, and  $\text{CH}_4$  emissions (Table 6, Fig. 8), but the magnitude of the increase was much larger for  $\text{CH}_4$  emissions ( $15.40\% \pm$

TABLE 6. Effects of LCC region, changes in air temperature ( $d\text{Tair}$ ), and their interaction on projection period (2010–2099) relative changes in net primary productivity ( $d\text{NPP}$ ), heterotrophic respiration ( $d\text{HR}$ ), and biogenic methane ( $d\text{BioCH}_4$ ).

Variable and effect	<i>n</i>	MS	<i>F</i>	<i>P</i>
<b><math>d\text{NPP}</math></b>				
$d\text{Tair}$	1	1,615.41	12.38	0.001
LCC	4	290.33	4.09	0.009
$d\text{Tair} \times \text{LCC}$	3	250.00	5.76	0.003
<b><math>d\text{HR}</math></b>				
$d\text{Tair}$	1	1,734.32	11.28	0.002
LCC	4	229.69	1.94	ns
$d\text{Tair} \times \text{LCC}$	3	227.46	3.49	0.027
<b><math>d\text{BioCH}_4</math></b>				
$d\text{Tair}$	1	16,349.57	27.52	<0.001
LCC	4	430.06	1.24	ns
$d\text{Tair} \times \text{LCC}$	3	1,812.70	3.51	0.027
<b><math>d\text{NPP}</math></b>				
$d\text{VWC}$	1	40.23	0.08	ns
LCC	4	63.32	1.65	ns
$d\text{VWC} \times \text{LCC}$	3	272.40	7.09	0.012
<b><math>d\text{HR}</math></b>				
$d\text{VWC}$	1	1,014.18	22.09	0.002
LCC	4	54.60	1.19	ns
$d\text{VWC} \times \text{LCC}$	3	282.78	6.16	0.018
<b><math>d\text{BioCH}_4</math></b>				
$d\text{VWC}$	1	15,010.09	13.05	0.007
LCC	4	11,296.65	2.46	ns
$d\text{VWC} \times \text{LCC}$	3	9457.65	2.74	ns

Notes: MS, mean square of *F* test; *F*, Fisher value; *P*, probability; ns, not significant. Change in precipitation, relative humidity, and net radiation had no significant effect on the three variables.

$3.04\%$  per  $^\circ\text{C}$  increase) than for NPP and HR ( $1.01\% \pm 1.84\%$  and  $1.67\% \pm 1.79\%$  per  $^\circ\text{C}$  increase, respectively). The interaction between LCC and temperature change was significant for all three variables, suggesting that the slope of the relationship between change in C fluxes and climate warming was significantly different among LCC regions (Table 6). The response of NPP and HR to warming was higher for the Arctic and North Pacific LCCs than for the Northwest Boreal and the Western Alaska LCCs (Fig. 8a, c). In contrast, the response of biogenic  $\text{CH}_4$  emissions was highest in the Northwest Boreal LCC (Fig. 8e). Soil moisture had a significantly positive effect on heterotrophic respiration and  $\text{CH}_4$  emissions (Fig. 8d, f),  $1.83\% \pm 0.78\%$  and  $10.93\% \pm 2.02\%$  per  $0.01 \text{ m}^3/\text{m}^3$  increase, respectively (Table 6). The sensitivity of HR to soil moisture was greatest in the North Pacific LCC, and least in the Northwest boreal LCC (Fig. 8d).

#### Biogeochemical processes affected by changing in fire regime

Compared to constant fire regime, the increase in fire frequency (and associated area burned) caused a significant decrease in NPP and HR of  $11.18\% \pm 2.33\%$  and  $40.36\% \pm 24.17\%$  per 10% increase in area burned, respectively (Table 7, Fig. 9a, b). In contrast, fire emissions increased with area burned at a rate of  $68.21 \pm 18.27 \text{ g C}\cdot\text{m}^{-2}\cdot\text{yr}^{-1}$  with 10% increase in area burned. The relationship between

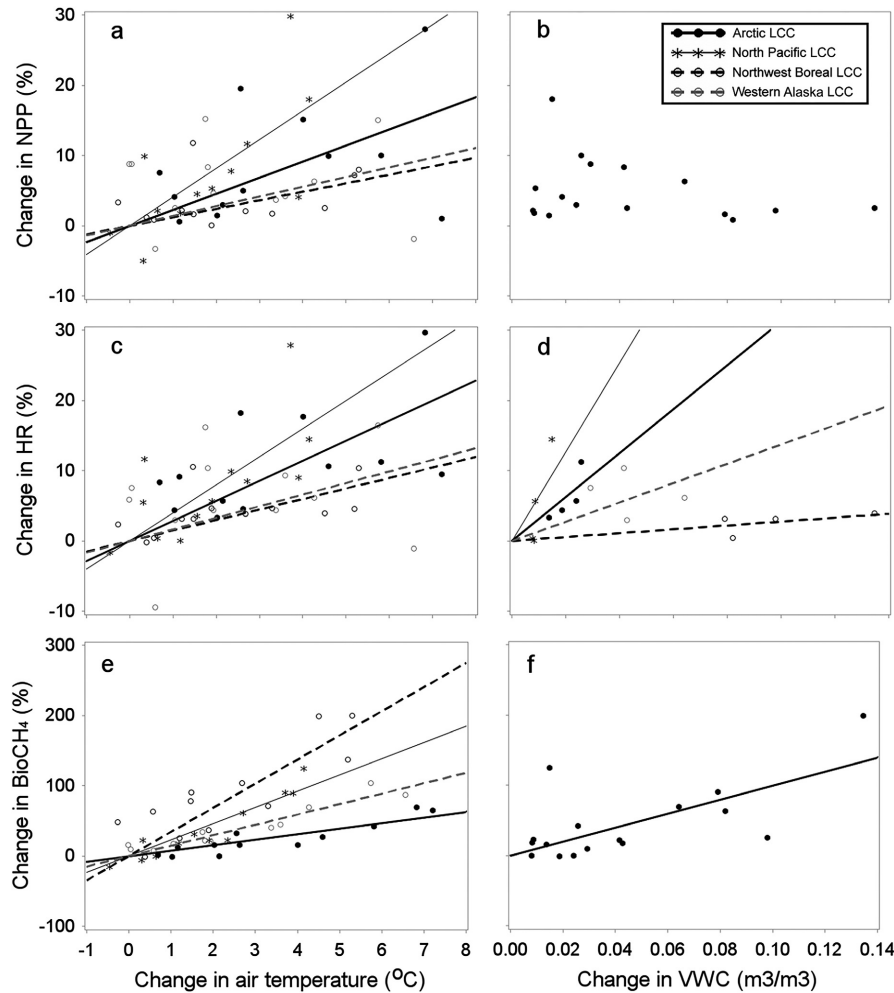


FIG. 8. Relationship between relative change in (a, b) NPP, (c, d) HR, and (e, f) BioCH<sub>4</sub> and (a, c, e) change in air temperature and (b, d, f) change in organic layer soil moisture. Different symbols and lines are depicted for each different LCC region. Each point represents the difference of decadal averages. The lines represent the linear relationships for each LCC.

fire emissions and area burned was significantly different among LCC regions (Fig. 9d); the slope of the relationship was lowest in the Northwest Boreal LCC. Although biogenic CH<sub>4</sub> emissions were not significantly affected by increasing area burned (Table 7), large increases in area burned (i.e., >4%) were associated with a decrease of biogenic CH<sub>4</sub> (Fig. 9d) that was approximately offset by increases in pyrogenic CH<sub>4</sub> (Fig. 9d).

#### DISCUSSION

Although wetland ecosystems cover only 12% of the terrestrial land surface in Alaska, they play an important role in the C dynamics of the state because they can emit substantial amounts of CH<sub>4</sub> to the atmosphere. This study focused on estimating the historical and future C dynamics of wetland ecosystems in Alaska using a modeling framework that coupled three models, ALFRESCO, DOS-TEM, and MDM-TEM. It is important to note that the modeling framework used in this assessment kept land cover static throughout the simulations. Future studies may therefore benefit by incorporating land surface and subsurface

dynamics into a similar modeling framework. Below, we first discuss changes in C dynamics of wetland ecosystems in Alaska during the historical and the projection periods of the simulations. We then discuss the relative importance of factors driving the dynamics of C in these simulations.

#### *Historical C dynamics in Alaska wetlands*

Alaska wetlands were estimated to store 5.56 Pg C in 2009, almost 90% of which was in the soil. Soil C pools of Alaska wetlands were estimated for the organic horizons and the top 1 m of mineral soil. The estimated soil organic C density was 27.9 kg C/m<sup>2</sup>, which is within the range of C density estimated from 1-m soil samples collected across wetlands in Alaska from the International Soil Carbon Database between 25.6 and 44.2 kg C/m<sup>2</sup> (Johnson et al. 2011). The estimated soil organic C density is also close to densities observed in the Alaska Beaufort Sea coast of  $21.2 \pm 3.8$  kg C/m<sup>2</sup>, collected from soil samples at depth between 55 and 260 cm (Ping et al. 2011, Hugelius et al. 2014), and  $25.8 \pm 18.8$  kg C/m<sup>2</sup> observed near Yukon River in central Alaska (Tarnocai et al. 2009, Hugelius et al.

TABLE 7. Effects of LCC region, changes in annual area burned (dAOB), and their interaction on projection period (2010–2099) relative changes in net primary productivity (dNPP), heterotrophic respiration (dHR), biogenic methane (dBioCH<sub>4</sub>), and total fire emission (dPyro).

Variable and effect	<i>n</i>	MS	<i>F</i>	<i>P</i>
<b>dNPP</b>				
dAOB	1	1.33	5.56	0.026
LCC	4	0.36	1.53	ns
dAOB × LCC	3	0.45	1.87	ns
<b>dHR</b>				
dAOB	1	145.19	8.93	0.006
LCC	4	15.51	0.81	ns
dAOB × LCC	3	30.11	1.74	ns
<b>dBioCH<sub>4</sub></b>				
dAOB	1	123.95	0.28	ns
LCC	4	1457.60	2.12	ns
dAOB × LCC	3	64.85	0.08	ns
<b>dPyro</b>				
dAOB	1	36134.63	102.41	<0.001
LCC	4	1620.47	4.09	0.01
dAOB × LCC	3	8436.14	24.22	<0.001

Note: MS, mean square of *F* test; *F*, Fisher value; *P*, probability; ns, not significant.

2014). The regional differences between the Arctic and boreal regions were also consistent with previous studies. Estimates of soil C density were 46.2 kg C/m<sup>2</sup> for the Arctic and Western Alaska LCCs, and 21.2 kg C/m<sup>2</sup> for the Northwest Boreal LCC. The lower C density in boreal compared to tundra regions was also reported in the circumpolar synthesis from Bradshaw and Warkentin (2015) where C density estimated down to 1 m was 36.9 and 16.0 kg C/m<sup>2</sup> for tundra and boreal peatlands, respectively. The greatest

uncertainties in the wetland C stocks estimates of this study are associated with (1) the depth of soil column and (2) the definition of wetland area. Our model simulations include the organic soil horizons and the top 1 m of the mineral soil horizon. It is important to recognize that soil organic C density in the northern permafrost region increases from 30 to 100 kg C/m<sup>2</sup> for estimates that consider soil depths of 1 and 3 m, respectively (Schuur et al. 2015).

While three out of the four LCC regions accumulated C during the historical period, our analysis indicated that the loss from the Northwest Boreal LCC was great enough to result in a statewide loss of 2.91 Tg C/yr. The loss of C from the Northwest Boreal LCC was mainly driven by the combination of HR and fire disturbance. The weak accumulation of C in the tundra and maritime forest regions of the state was primarily driven by the fact that increases in NPP were slightly larger than increases in HR. We estimated that historical annual NPP from Alaska wetlands was about 205 g C·m<sup>-2</sup>·yr<sup>-1</sup> (ranging from 135 g C·m<sup>-2</sup>·yr<sup>-1</sup> in the Arctic LCC to 269 g C·m<sup>-2</sup>·yr<sup>-1</sup> in the North Pacific LCC), which is generally consistent with average annual NPP estimated in northern peatlands. For example, the Arctic LCC NPP estimate is consistent with observation-based estimates of NPP in arctic wet sedge tundra in Alaska of 75–160 g C·m<sup>-2</sup>·yr<sup>-1</sup> based on GPP estimates of Euskirchen et al. (2016a) from 2008 through 2015, assuming that NPP is 50% of GPP. This estimate was also similar to the estimates of 69 g C·m<sup>-2</sup>·yr<sup>-1</sup> and 158 g C·m<sup>-2</sup>·yr<sup>-1</sup> estimated by Shaver and Chapin (1991) for aboveground vegetation of wet sedge tundra and moist tussock tundra, respectively.

CH<sub>4</sub> emissions of Alaska wetlands were primarily derived from biogenic sources, with statewide mean biogenic CH<sub>4</sub> emissions of 0.91 Tg C/yr and mean pyrogenic CH<sub>4</sub> emissions of 0.02 Tg C/yr during the historical period. The

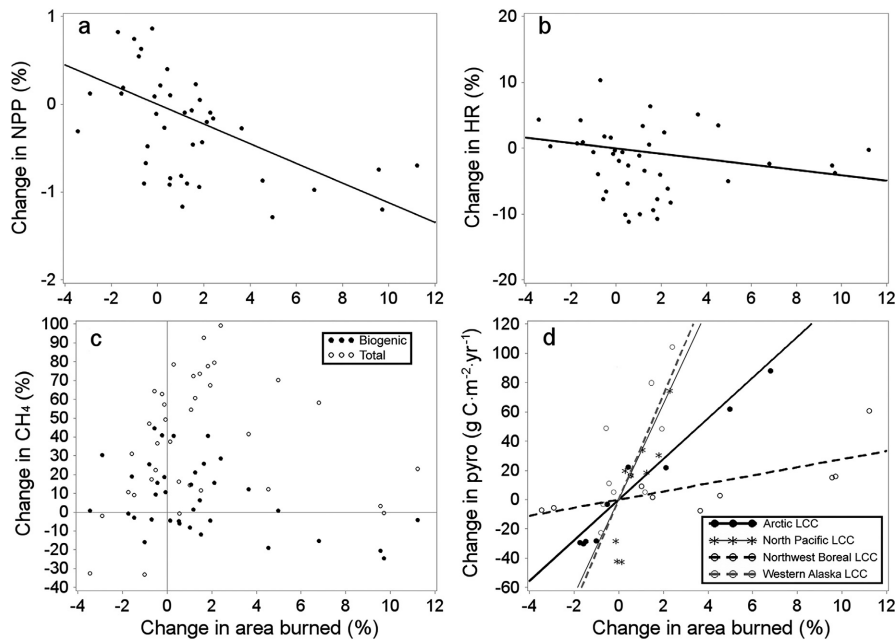


FIG. 9. Relationship between relative change in (a) NPP, (b) HR, (c) BioCH<sub>4</sub> and total CH<sub>4</sub> (including pyrogenic CH<sub>4</sub>), and (d) total fire emissions (pyro) and change in area burned. Different symbols and lines are depicted for each different LCC region. Each point represents the difference of decadal averages. The lines represent the linear relationships for each LCC.

historical estimates of biogenic CH<sub>4</sub> emissions in the Arctic LCC (2.5 g C·m<sup>-2</sup>·yr<sup>-1</sup>) were close to 2012/2014 flux tower estimates from Barrow, Alaska (3.1 g C·m<sup>-2</sup>·yr<sup>-1</sup>; Karion et al. 2016). Similarly, the historical estimates of biogenic CH<sub>4</sub> emissions in the Northwest Boreal LCC (6.0 g C·m<sup>-2</sup>·yr<sup>-1</sup>) were close to estimates from Whalen and Reeburgh (1988, 1992) collected at a tussock tundra sites in Interior Alaska (1.5 to 18.9 g C·m<sup>-2</sup>·yr<sup>-1</sup> from 1987 to 1990). Statewide, biogenic CH<sub>4</sub> emissions from wetlands (5.8 g C·m<sup>-2</sup>·yr<sup>-1</sup>, excluding the North Pacific LCC) were comparable to previous model estimates from McGuire et al. (2012; 8.9 g C·m<sup>-2</sup>·yr<sup>-1</sup>) for the Bering Strait and Chukchi Sea regions.

Statewide historical GWP during the historical period was estimated to be 37.16 Tg CO<sub>2</sub>-eq/yr. It was driven by the large GWP estimated in the Northwest Boreal LCC that was the result of CO<sub>2</sub> loss from HR and fire emissions and substantial pyrogenic and biogenic CH<sub>4</sub> emissions. Biogenic CH<sub>4</sub> emissions of this region were substantially higher compared to those of the colder tundra wetland regions (the Arctic and Western Alaska LCCs) because of greater wetland area as well as warmer soils and longer growing seasons. The large fire emissions resulted from the active fire regime at play in the region. From 1950 to 2009, the annual area burned in the Northwest Boreal LCC was 3,262 km<sup>2</sup>, which is more than 85% of the statewide area burned (Zhu and McGuire 2016).

The net C sequestration observed in the Arctic and the North Pacific LCCs (NECB of 0.54 Tg C/yr) was more than offset by the higher GWP of biogenic CH<sub>4</sub> emissions, resulting in a positive GWP of 0.64 Tg CO<sub>2</sub>-eq/yr. The Western Alaska LCC was the only region for which a negative GWP was calculated. Wetlands in this region are dominated by wet sedge tundra, which is more productive than tussock tundra (Euskirchen et al. 2016a). As a result, biogenic CH<sub>4</sub> emissions were not enough to offset the net C sequestration, resulting in a GWP of -0.15 Tg CO<sub>2</sub>-eq/yr.

#### *Future C dynamics in Alaska wetlands*

Our analysis indicated that wetlands in Alaska will gain C by the end of this century, with increases of 4.2–8.1% among the scenarios we considered, compared to the end of the historical period. This C sequestration was primarily driven by the stronger increase of NPP over HR, fire emissions, and CH<sub>4</sub> emissions. The increase of NPP was driven by the increase in atmospheric CO<sub>2</sub> (i.e., CO<sub>2</sub> fertilization effect) and the increase in air temperature, although the rate of response was modest (5.2% ± 0.21% per 100 ppmv [mean ± SE] increase and 1.0% ± 1.84% per °C increase at statewide level, respectively) in comparison with data-based and model-based estimates. For example, based on FACE experiments in temperate forests, Norby et al. (2005) estimated that NPP increases 13% per 100 ppmv increase of atmospheric CO<sub>2</sub>. Piao et al. (2013) calculated that NPP increased 16% per 100 ppmv increase of atmospheric CO<sub>2</sub> based on multi-model simulations. The temperature sensitivity of NPP has been reported to increase 1–2% per °C increase in warming experiments conducted at a Minnesota wetland site (Piao et al. 2013; Fig. 4). It has been suggested that overestimation of the effects of elevated CO<sub>2</sub> on

ecosystem production by models may be due to lack of nitrogen limitation by models (Hungate et al. 2003, McGuire et al. 2016). The simulations in this study considered the effects of N limitation on C assimilation.

Our analysis indicated that the response of NPP to increases in CO<sub>2</sub> became less sensitive as the atmospheric CO<sub>2</sub> level increased (Fig. 7a). The response of NPP to increasing air temperature was in part associated with longer growing seasons due to later onset of snowfall and earlier spring snowmelt consistent with previous studies (Sharratt 1992, Keeling et al. 1996, Randerson et al. 1999, Starr et al. 2000, Euskirchen et al. 2006, 2016b, Déry and Brown 2007, Piao et al. 2007, Brown et al. 2010). Several remote sensing records and modeling studies have also documented the positive effect of warmer temperatures and elevated atmospheric CO<sub>2</sub> on ecosystem NPP through enhanced plant growth from prolonged growing season and increased nutrient input (Koch and Mooney 1996, Schulze et al. 1999, Shaver et al. 2000), which supports our analysis. These seasonal changes were more influential in the Arctic and the North Pacific LCC than the other LCCs in Alaska. The high sensitivity of NPP to warming in the Arctic LCC was likely associated with the fact that the Arctic LCC is the coldest LCC, where temperature is an important limiting factor for plant growth. The high sensitivity of NPP to warming in the North Pacific LCC was likely driven by the increasing length in the growing season, as the region shows the largest change in snow melt and snow return dynamics in response to warming (Genet et al. 2017; Fig. 8). The increase in HR was also caused by both increasing atmospheric CO<sub>2</sub> and rising air temperature, consistent with previous studies (Norby et al. 2001, Kimball et al. 2004, Pendall et al. 2004). Rising air temperature directly increased soil temperature, which can enhance rates of microbial decomposition. In addition, rising air temperature together with increasing CO<sub>2</sub> levels promoted higher vegetation productivity and litterfall, which increased the absolute and relative quantities of active C pools to increase HR. Increases in HR occurred in response to increase in atmospheric CO<sub>2</sub>, and followed a downward curvilinear relationship (Fig. 7b), indicating that the effects of CO<sub>2</sub> fertilization on HR will ultimately saturate. While both NPP and HR increased in response to increase in CO<sub>2</sub> and temperature, studies have suggested that the overall effect may depend on soil moisture dynamics, thawing of the permafrost, and C:N ratio (Pendall et al. 2004, Sitch et al. 2007). The simulations in this study show an overall increase in soil moisture in response to projected climate change. This increase in soil moisture caused an increase in HR, as a likely consequence of the positive effect of soil moisture on permafrost thaw and the exposure of previously frozen soil C (the change in active layer depth was significantly and positively correlated to change in soil moisture;  $n = 35$ ,  $F = 24.12$ ,  $P < 0.01$ ). The increase in soil moisture in the projected period indicates that the responses of NPP and HR to atmospheric CO<sub>2</sub> were likely not limited by drought stress in our simulations. The increase in fire disturbance significantly decreased NPP due to substantial vegetation mortality following fire. Fire can also result in reduced HR and biogenic CH<sub>4</sub> emissions due to partially or entirely combusted C rich organic layers and associated microbial communities. The net effect of fire regime on the

C balance in our study was a decrease in NECB and C release to the atmosphere from both the vegetation and the soil C pools.

Biogenic CH<sub>4</sub> emissions are the major sources of CH<sub>4</sub> from Alaska wetlands to the atmosphere. Our simulations projected an average 47.7% increase in CH<sub>4</sub> emissions during the projection period among the climate scenarios we considered. The long-term response of CH<sub>4</sub> emissions to climate change in our simulations is comparable to the 7–35% projected increases under RCP 4.5 and RCP8.5 scenarios in the northern permafrost region during 2010–2100 by other models (Koven et al. 2015), yet significantly less than the twofold increase simulated by Zhuang et al. (2006). However, the positive effect of warming on CH<sub>4</sub> emissions might be overestimated. Discrepancies between long-term and short-term CH<sub>4</sub> emissions sensitivity have been suggested by the analysis of long-term CH<sub>4</sub> concentration measurements in Barrow, Alaska (Sweeney et al. 2016). These data indicate that (1) the short-term sensitivity of CH<sub>4</sub> emissions to air temperature may not play out over longer time periods and (2), at larger spatial scales, other environmental drivers are controlling longer term and spatial dynamics of CH<sub>4</sub>.

Increasing atmospheric CO<sub>2</sub> resulted in a minor increase in CH<sub>4</sub> emissions (1.5% ± 0.09% per 100 ppmv increase at statewide level) through the increased litterfall associated with the increase in vegetation productivity. The increase in litterfall resulted in an increase in decomposable C available for methanogenesis (Hutchin et al. 1995, Saarnio and Silvola 1999, Saarnio et al. 2003). In contrast, increasing air temperature had a large effect on CH<sub>4</sub> emissions (15.4% ± 3.0% per °C increase at statewide level), primarily due to the additional direct effect of warming soil temperature on accelerated anaerobic decomposition. The positive response of CH<sub>4</sub> emissions to increasing air temperature is supported by recent studies suggesting that terrestrial high-latitude CH<sub>4</sub> emissions are more impacted by changes in temperature than by increased availability of organic matter (Updegraff et al. 2001, Turetsky et al. 2008, Olefeldt et al. 2013, Ma et al. 2017).

In general, increases in wildfire frequency caused decreases in biogenic CH<sub>4</sub> emissions because of decreases in NPP and the combustion of the soil organic horizons. Vegetation can influence soil C dynamics by the exudation of C compounds into the rhizosphere that fuel methanogenesis (Schimel 1995, King and Reeburgh 2002, Chanton et al. 2008). This process is represented in MDM-TEM, in which monthly NPP is used as an indicator of the temporal and spatial variability of root exudates available for methanogenesis (Zhuang et al. 2004). However, the negative effect of wildfire was more than offset by the positive effect of increasing air temperature and, to a minor extent, increases in atmospheric CO<sub>2</sub>.

Changes in fire regime had negative effects on GWP in this study. Our attribution analysis revealed that this slight decrease in biogenic CH<sub>4</sub> emissions in response to fire was not enough to compensate for the decrease in C sequestration and the increase in pyrogenic CH<sub>4</sub> emissions. However, CH<sub>4</sub> emissions in our analysis were not directly affected by the availability of newly thawed soil C exposed by the permafrost thaw. Field observations have shown that CH<sub>4</sub> emissions increase in boreal peatlands following thaw (Johnston

et al. 2014). This response of CH<sub>4</sub> emissions could reverse the negative effects of changing fire regime on GWP, as the release of 2.3% of permafrost C emissions as CH<sub>4</sub>, could increase warming potential by 35%–48% over the remainder of this century (Schuur et al. 2015, see also Frohling et al. 2011). Furthermore, our analysis suggests that the decreasing sensitivity of NPP to atmospheric CO<sub>2</sub>, the linear increase in biogenic CH<sub>4</sub> emissions to air temperature, in addition to the increase in pyrogenic CH<sub>4</sub> emissions and C loss from wildfires may lead to an overall increase in GWP beyond 2100 (see also McGuire et al. 2018).

The transitions of wetlands in Alaska from being a source of atmospheric CO<sub>2</sub> in the historical period to a sink during the remainder of the 21st century in our analysis, and the possibility of becoming a C source beyond 2100, emphasizes the changing influence of multiple driving factors in shaping the C dynamics of wetlands in Alaska. The inferred transition of C dynamics of wetlands in Alaska to becoming a source of C to the atmosphere beyond 2100 we believe will be driven by a decreasing sensitivity of NPP to increasing CO<sub>2</sub>, an increasing availability of soil C for decomposition as permafrost thaws, and a linear sensitivity of biogenic CH<sub>4</sub> emissions to increasing soil temperature.

## CONCLUSION

This study, which assessed C dynamics in wetlands in Alaska during the historical period from 1950 to the end of 2009 and the rest of 21st century, indicates that wetlands will play an important role in response of the regional C dynamics to changing climate, atmospheric CO<sub>2</sub>, and fire regime. Our analysis suggests that wetland ecosystems of Alaska lost C during 1950–2009, but that they will sequester C during the remainder of this century. The analysis also indicates that even though the ecosystem CO<sub>2</sub> sequestration more than offset C loss from HR and fire emissions, GWP will remain positive because of substantial CH<sub>4</sub> emissions from wetlands. Although our analysis indicates that GWP will weaken somewhat during the 21st century, beyond 2100, we expect that GWP will ultimately increase as wetland ecosystems transition from being a sink to a source of atmospheric CO<sub>2</sub> because of the decreasing sensitivity of NPP to increasing CO<sub>2</sub>, the increasing availability of soil C for decomposition as permafrost thaws, and the linear sensitivity of biogenic CH<sub>4</sub> emissions to increase in soil temperature.

## ACKNOWLEDGMENTS

This research was funded by the U.S. Geological Survey (USGS) Land Change Science Program. Additional support was provided by the Alaska Climate Science Center through Grant/Cooperative Agreement G10AC00588 from the U.S. Geological Survey and by the Bonanza Creek Long-Term Ecological Research Program funded by the National Science Foundation and the U.S. Forest Service. The research was also partially supported by DOE project DE-SC0008092 and NSF project IIS-1027955 to Q. Zhuang. Any use of trade, firm, or product names is for descriptive purposes only and does not imply endorsement by the U.S. Government. We acknowledge the World Climate Research Programme's Working Group on Coupled Modeling, which is responsible for CMIP, and we thank all the climate modeling groups for producing and making available their model output. We also thank the U.S. Department of Energy's Program for Climate Model Diagnosis and Intercomparison for providing coordinating support and leading development of

software infrastructure in partnership with the Global Organization for Earth System Science Portals.

## LITERATURE CITED

- Alexeev, V. A. 2003. Sensitivity to CO<sub>2</sub> doubling of an atmospheric GCM coupled to an oceanic mixed layer: a linear analysis. *Climate Dynamics* 20:775–787.
- Alexeev, V. A., P. L. Langen, and J.R. Bates. 2005. Polar amplification of surface warming on an aquaplanet in “ghost forcing” experiments without sea ice feedbacks. *Climate Dynamics* 24:655–666.
- Bradshaw, C. J., and I. G. Warkentin. 2015. Global estimates of boreal forest carbon stocks and flux. *Global and Planetary Change* 128:24–30.
- Brown, R., C. Derksen, and L. Wang. 2010. A multi-data set analysis of variability and change in Arctic spring snow cover extent, 1967–2008. *Journal of Geophysical Research–Atmospheres* 115: D16111, <https://doi.org/10.1029/2010JD013975>
- Burkett, V., and J. Kusler. 2000. Climate change: potential impacts and interactions in wetlands of the United States I. *JAWRA Journal of the American Water Resources Association* 36:313–320.
- Cai, M. 2006. Dynamical greenhouse-plus feedback and polar warming amplification. Part I: a dry radiative-transportive climate model. *Climate Dynamics* 26:661–675.
- Cai, M., and J. Lu. 2007. Dynamical greenhouse-plus feedback and polar warming amplification. Part II: Meridional and vertical asymmetries of the global warming. *Climate Dynamics* 29:375–391.
- Chanton, J. P., P. H. Glaser, L. S. Chasar, D. J. Burdige, M. E. Hines, D. I. Siegel, L. B. Tremblay, and W. T. Cooper. 2008. Radiocarbon evidence for the importance of surface vegetation on fermentation and methanogenesis in contrasting types of boreal peatlands. *Global Biogeochemical Cycles* 22:GB4022, <https://doi.org/10.1029/2008GB003274>
- Chapin, F. S., et al. 2006. Reconciling carbon-cycle concepts, terminology, and methods. *Ecosystems* 9:1041–1050.
- Crill, P. M., K. B. Bartlett, R. C. Harriss, E. Gorham, E. S. Verry, D. I. Sebacher, L. Madzar, and W. Sanner. 1988. Methane flux from Minnesota peatlands. *Global Biogeochemical Cycles* 2:371–384.
- Déry, S. J., and R. D. Brown. 2007. Recent Northern Hemisphere snow cover extent trends and implications for the snow-albedo feedback. *Geophysical Research Letters* 34:L22504, <https://doi.org/10.1029/2007GL031474>
- Development Assistance Committee Organisation for Economic Co-operation and Development. 1996. Guidelines for aid agencies for improved conservation and sustainable use of tropical and sub-tropical wetlands. OECD, Paris, France.
- Dlugokencky, E. J., K. A. Masarie, P. M. Lang, and P. P. Tans. 1998. Continuing decline in the growth rate of the atmospheric methane burden. *Nature* 393:447–450.
- Euskirchen, E. S., et al. 2006. Importance of recent shifts in soil thermal dynamics on growing season length, productivity, and carbon sequestration in terrestrial high-latitude ecosystems. *Global Change Biology* 12:731–750.
- Euskirchen, E. S., M. S. Bret-Harte, G. R. Shaver, C. W. Edgar, and V. E. Romanovsky. 2016a. Long-term release of carbon dioxide from arctic tundra ecosystems in Alaska. *Ecosystems* 20:960–974.
- Euskirchen, E. S., A. P. Bennett, A. L. Breen, H. Genet, M. A. Lindgren, T. A. Kurkowski, A. D. McGuire, and T. S. Rupp. 2016b. Consequences of changes in vegetation and snow cover for climate feedbacks in Alaska and northwest Canada. *Environmental Research Letters* 11:105003.
- Fao, I., and I. Isric. 2012. JRC: harmonized world soil database (version 1.2). FAO, Rome, Italy and IIASA, Laxenburg, Austria.
- Fiedler, S., and M. Sommer. 2000. Methane emissions, groundwater levels and redox potentials of common wetland soils in a temperate-humid climate. *Global Biogeochemical Cycles* 14:1081–1093.
- Fisher, J. B., et al. 2014. Carbon cycle uncertainty in the Alaskan Arctic. *Biogeosciences* 11:4271–4288.
- Forster, P. D. F., M. Blackburn, R. Glover, and K. P. Shine. 2000. An examination of climate sensitivity for idealised climate change experiments in an intermediate general circulation model. *Climate Dynamics* 16:833–849.
- Forster, P., et al. 2007. Changes in atmospheric constituents and in radiative forcing. Chapter 2 in *Climate Change 2007. The Physical Science Basis*. Cambridge University Press, Cambridge, UK.
- French, N. H., E. S. Kasichke, and D. G. Williams. 2002. Variability in the emission of carbon-based trace gases from wildfire in the Alaskan boreal forest. *Journal of Geophysical Research: Atmospheres* 107(D1):8146. <https://doi.org/10.1029/2001jd000480>.
- Frolking, S., J. Talbot, M. C. Jones, C. C. Treat, J. B. Kauffman, E. S. Tuittila, and N. Roulet. 2011. Peatlands in the Earth’s 21st century climate system. *Environmental Reviews* 19:371–396.
- Fung, I., J. John, J. Lerner, E. Matthews, M. Prather, L. P. Steele, and P. J. Fraser. 1991. Three-dimensional model synthesis of the global methane cycle. *Journal of Geophysical Research–Atmospheres* 96:13033–13065.
- Genet, H., Y. He, A. D. McGuire, Q. Zhuang, Y. Zhang, F. Biles, D. V. D’Amore, K. Zhou and K. D. Johnson. 2016. Terrestrial carbon modeling: baseline and projections in upland ecosystems. Pages 105–132 in *Baseline and projected future carbon storage and greenhouse-gas fluxes in ecosystems of Alaska*. US Geological Survey, Reston, Virginia, USA.
- Genet, H., et al. 2017. The role of driving factors in historical and projected carbon dynamics of upland ecosystems in Alaska. *Ecological Applications* 28:5–27.
- Global Soil Data Task Group. 2000. Global gridded surfaces of selected soil characteristics (IGBP-DIS). ORNL Distributed Active Archive Center, Oak Ridge National Laboratory, Oak Ridge, Tennessee, USA.
- Graversen, R. G., and M. Wang. 2009. Polar amplification in a coupled climate model with locked albedo. *Climate Dynamics* 33:629–643.
- Gustine, D. D., T. J. Brinkman, M. A. Lindgren, J. I. Schmidt, T. S. Rupp, and L. G. Adams. 2014. Climate-driven effects of fire on winter habitat for caribou in the Alaskan-Yukon Arctic. *PLoS ONE* 9:e100588.
- Harris, I. P. D. J., P. D. Jones, T. J. Osborn, and D. H. Lister. 2014. Updated high-resolution grids of monthly climatic observations—the CRU TS3. 10 Dataset. *International Journal of Climatology* 34:623–642.
- Hartmann, B., and G. Wendler. 2005. The significance of the 1976 Pacific climate shift in the climatology of Alaska. *Journal of Climate* 18:4824–4839.
- He, Y., H. Genet, A. D. McGuire, Q. Zhuang, B. Wylie, and Y. Zhang. 2016. Terrestrial carbon modeling: baseline and projections in lowland ecosystems of Alaska. Pages 133–158 in *Baseline and projected future carbon storage and greenhouse-gas fluxes in ecosystems of Alaska*. US Geological Survey, Reston, Virginia, USA.
- Hugelius, G., et al. 2014. Estimated stocks of circumpolar permafrost carbon with quantified uncertainty ranges and identified data gaps. *Biogeosciences* 11:6573–6593.
- Hungate, B. A., J. S. Dukes, M. R. Shaw, Y. Luo, and C. B. Field. 2003. Nitrogen and climate change. *Science* 302:1512–1513.
- Hutchin, P. R., M. C. Press, J. A. Lee, and T. W. Ashenden. 1995. Elevated concentrations of CO<sub>2</sub> may double methane emissions from mires. *Global Change Biology* 1:125–128.
- IPCC, Climate Change. 2014. Mitigation of Climate Change. Contribution of Working Group III to the Fifth Assessment Report of the Intergovernmental Panel on Climate Change. Cambridge University Press, Cambridge, UK.
- Johnson, K. D., et al. 2011. Soil carbon distribution in Alaska in relation to soil-forming factors. *Geoderma* 167:71–84.
- Johnston, C. E., S. A. Ewing, J. W. Harden, R. K. Varner, K. P. Wickland, J. C. Koch, C. C. Fuller, K. Manies, and M. T. Jorgenson. 2014. Effect of permafrost thaw on CO<sub>2</sub> and CH<sub>4</sub> exchange

- in a western Alaska peatland chronosequence. *Environmental Research Letters* 9:085004.
- Johnstone, J. F., T. S. Rupp, M. Olson, and D. Verbyla. 2011. Modeling impacts of fire severity on successional trajectories and future fire behavior in Alaskan boreal forests. *Landscape Ecology* 26:487–500.
- Kaplan, J. O., and M. New. 2006. Arctic climate change with a 2°C global warming: Timing, climate patterns and vegetation change. *Climatic Change* 79:213–241.
- Karion, A., et al. 2016. Investigating Alaskan methane and carbon dioxide fluxes using measurements from the CARVE tower. *Atmospheric Chemistry and Physics* 16:5383–5398.
- Kasischke, E. S., and M. R. Turetsky. 2006. Recent changes in the fire regime across the North American boreal region—spatial and temporal patterns of burning across Canada and Alaska. *Geophysical Research Letters* 33:L09703. <https://doi.org/10.1029/2006GL025677>
- Kasischke, E. S., D. Williams, and D. Barry. 2002. Analysis of the patterns of large fires in the boreal forest region of Alaska. *International Journal of Wildland Fire* 11:131–144.
- Keeling, C. D., J. F. S. Chin, and T. P. Whorf. 1996. Increased activity of northern vegetation inferred from atmospheric CO<sub>2</sub> measurements. *Nature* 382:146.
- Kimball, J. S., K. C. McDonald, S. W. Running, and S. E. Frolking. 2004. Satellite radar remote sensing of seasonal growing seasons for boreal and subalpine evergreen forests. *Remote Sensing of Environment* 90:243–258.
- King, J. Y., and W. S. Reeburgh. 2002. A pulse-labeling experiment to determine the contribution of recent plant photosynthates to net methane emission in arctic wet sedge tundra. *Soil Biology and Biochemistry* 34:173–180.
- King, J., W. Reeburgh and S. Regli. 1998. Methane flux data, Alaska North Slope, 1994–1996, report. National Snow and Ice Data Center, Boulder, Colorado, USA. <http://nsidc.org/data/arcs013.html>
- Kirschke, S., et al. 2013. Three decades of global methane sources and sinks. *Nature Geoscience* 6:813–823.
- Koch, G. W., and H. A. Mooney. 1996. Response of terrestrial ecosystems to elevated CO<sub>2</sub>: a synthesis and summary. Pages 415–429 in G. W. Koch and H. A. Mooney, editors. *Carbon dioxide and terrestrial ecosystems*. Academic Press, San Diego, California, USA.
- Koven, C. D., B. Ringeval, P. Friedlingstein, P. Ciais, P. Cadule, D. Khvorostyanov, G. Krinner, and C. Tarnocai. 2011. Permafrost carbon-climate feedbacks accelerate global warming. *Proceedings of the National Academy of Sciences USA* 108:14769–14774.
- Koven, C. D., et al. 2015. A simplified, data-constrained approach to estimate the permafrost carbon–climate feedback. *Philosophical Transactions of the Royal Society A* 373:20140423.
- Langen, P. L., and V. A. Alexeev. 2007. Polar amplification as a preferred response in an idealized aquaplanet GCM. *Climate Dynamics* 29:305–317.
- Ma, S., J. Jiang, Y. Huang, Z. Shi, R. M. Wilson, D. Ricciuto, S. D. Sebestyen, P. J. Hanson, and Y. Luo. 2017. Data-constrained projections of methane fluxes in a Northern Minnesota Peatland in response to elevated CO<sub>2</sub> and warming. *Journal of Geophysical Research–Biogeosciences* 122:2841–2861.
- Manabe, S., and R. J. Stouffer. 1980. Sensitivity of a global climate model to an increase of CO<sub>2</sub> concentration in the atmosphere. *Journal of Geophysical Research–Oceans* 85:5529–5554.
- Mann, D. H., T. Scott Rupp, M. A. Olson, and P. A. Duffy. 2012. Is Alaska’s boreal forest now crossing a major ecological threshold? Arctic, Antarctic, and Alpine Research 44:319–331.
- Marchenko, S., V. Romanovsky and G. Tipenko. 2008. Numerical modeling of spatial permafrost dynamics in Alaska. Pages 1125–1130 in *Proceedings of the 9th International Conference on Permafrost* (Vol. 29). Institute of Northern Engineering, University of Alaska Fairbanks, Fairbanks, Alaska, USA.
- Matthews, E., and I. Fung. 1987. Methane emission from natural wetlands: Global distribution, area, and environmental characteristics of sources. *Global Biogeochemical Cycles* 1:61–86.
- McFarlane, N. A., G. J. Boer, J.-P. Blanchet, and M. Lazare. 1992. The Canadian climate centre second-generation general circulation model and its equilibrium climate. *Journal of Climate* 5:1013–1044.
- McGuire, A. D., F. S. Chapin III, J. E. Walsh, and C. Wirth. 2006. Integrated regional changes in arctic climate feedbacks: Implications for the global climate system. *Annual Review of Environment and Resources* 31:61–91.
- McGuire, A. D., L. G. Anderson, T. R. Christensen, S. Dallimore, L. Guo, D. J. Hayes, M. Heimann, T. D. Lorenson, R. W. Macdonald, and N. Roulet. 2009. Sensitivity of the carbon cycle in the Arctic to climate change. *Ecological Monographs* 79:523–555.
- McGuire, A. D., et al. 2012. An assessment of the carbon balance of Arctic tundra: comparisons among observations, process models, and atmospheric inversions. *Biogeosciences Discussions* 9:4543.
- McGuire, A. D., et al. 2016. Variability in the sensitivity among model simulations of permafrost and carbon dynamics in the permafrost region between 1960 and 2009. *Global Biogeochemical Cycles* 30:1015–1037.
- McGuire, A. D., et al. 2018. The dependence of the evolution of carbon dynamics in the northern permafrost region on the trajectory of climate change. *Proceedings of the National Academy of Sciences USA* 115:3882–3887.
- Meehl, G. A., C. Covey, K. E. Taylor, T. Delworth, R. J. Stouffer, M. Latif, B. McAvaney, and J. F. Mitchell. 2007. The WCRP CMIP3 multimodel dataset: A new era in climate change research. *Bulletin of the American Meteorological Society* 88:1383–1394.
- Minsley, B. J., N. J. Pastick, B. K. Wylie, D. Brown, and M. Andy Kass. 2016. Evidence for nonuniform permafrost degradation after fire in boreal landscapes. *Journal of Geophysical Research–Earth Surface* 121:320–335.
- Mishra, U., and W. J. Riley. 2012. Alaskan soil carbon stocks: spatial variability and dependence on environmental factors. *Biogeosciences* 9:3637–3645.
- Mondav, R., et al. 2014. Discovery of a novel methanogen prevalent in thawing permafrost. *Nature Communications* 5:3212.
- Nakicenovic, N., J. Alcamo, A. Grubler, K. Riahi, R. A. Roehrl, H. H. Rogner, and N. Victor. 2000. Special report on emissions scenarios (SRES), a special report of Working Group III of the intergovernmental panel on climate change. Cambridge University Press, Cambridge, UK.
- Newcomer, J., et al., editors. 2000. Collected data of the Boreal Ecosystem–Atmosphere Study [CD-ROM]. NASA Goddard Space Flight Center, Greenbelt, Maryland, USA.
- Norby, R. J., M. F. Cotrufo, P. Ineson, E. G. O’Neill, and J. G. Canadell. 2001. Elevated CO<sub>2</sub>, litter chemistry, and decomposition: a synthesis. *Oecologia* 127:153–165.
- Norby, R. J., et al. 2005. Forest response to elevated CO<sub>2</sub> is conserved across a broad range of productivity. *Proceedings of the National Academy of Sciences USA* 102:18052–18056.
- O’Donnell, J. A., J. W. Harden, A. D. McGuire, and V. E. Romanovsky. 2011. Exploring the sensitivity of soil carbon dynamics to climate change, fire disturbance and permafrost thaw in a black spruce ecosystem. *Biogeosciences Discussions* 7:8853–8893.
- Olefeldt, D., M. R. Turetsky, P. M. Crill, and A. D. McGuire. 2013. Environmental and physical controls on northern terrestrial methane emissions across permafrost zones. *Global Change Biology* 19:589–603.
- Olefeldt, D., E. S. Euskirchen, J. Harden, E. Kane, A. D. McGuire, M. P. Waldrop, and M. R. Turetsky. 2017. A decade of boreal rich fen greenhouse gas fluxes in response to natural and experimental water table variability. *Global Change Biology* 23:2428–2440.
- Pastick, N. J., M. T. Jorgenson, B. K. Wylie, S. J. Nield, K. D. Johnson, and A. O. Finley. 2015. Distribution of near-surface permafrost in Alaska: estimates of present and future conditions. *Remote Sensing of Environment* 168:15.
- Pastick, N., et al. 2017. Historical and projected trends in landscape drivers affecting carbon dynamics in Alaska. *Ecological Applications* 27:1383–1402.

- Pendall, E., et al. 2004. Below-ground process responses to elevated CO<sub>2</sub> and temperature: a discussion of observations, measurement methods, and models. *New Phytologist* 162:311–322.
- Piao, S., P. Friedlingstein, P. Ciais, N. Viovy, and J. Demarty. 2007. Growing season extension and its impact on terrestrial carbon cycle in the Northern Hemisphere over the past 2 decades. *Global Biogeochemical Cycles* 21:GB3018, <https://doi.org/10.1029/2006GB002888>
- Piao, S., et al. 2013. Evaluation of terrestrial carbon cycle models for their response to climate variability and to CO<sub>2</sub> trends. *Global Change Biology* 19:2117–2132.
- Ping, C. L., G. J. Michaelson, M. T. Jorgenson, J. M. Kimble, H. Epstein, V. E. Romanovsky, and D. A. Walker. 2008. High stocks of soil organic carbon in the North American Arctic region. *Nature Geoscience* 1:615.
- Ping, C. L., G. J. Michaelson, L. Guo, M. T. Jorgenson, M. Kanevskiy, Y. Shur, F. Dou, and J. Liang. 2011. Soil carbon and material fluxes across the eroding Alaska Beaufort Sea coastline. *Journal of Geophysical Research: Biogeosciences* 116:G02004, <https://doi.org/10.1029/2010JG001588>
- Randerson, J. T., C. B. Field, I. Y. Fung, and P. P. Tans. 1999. Increases in early season ecosystem uptake explain recent changes in the seasonal cycle of atmospheric CO<sub>2</sub> at high northern latitudes. *Geophysical Research Letters* 26:2765–2768.
- Reeburgh, W. S., and S. C. Whalen. 1992. High-Latitude Ecosystems as CH<sub>4</sub> Sources. *Ecological Bulletins* 42:62–70.
- Roeckner, E., R. Brokopf, M. Esch, M. Giorgetta, S. Hagemann, L. Kornblueh, E. Manzini, U. Schlese, and U. Schulzweida. 2004. The atmospheric general circulation model. Max Planck Institut für Meteorologie, Hamburg, Germany.
- Rupp, T. S., A. M. Starfield, and F. S. Chapin. 2000. A frame-based spatially explicit model of subarctic vegetation response to climatic change: comparison with a point model. *Landscape Ecology* 15:383–400.
- Rupp, T. S., A. M. Starfield, F. S. Chapin, and P. Duffy. 2002. Modeling the impact of black spruce on the fire regime of Alaskan boreal forest. *Climatic Change* 55:213–233.
- Rupp, T. S., X. Chen, M. Olson, and A. D. McGuire. 2007. Sensitivity of simulated boreal fire dynamics to uncertainties in climate drivers. *Earth Interactions* 11:1–21.
- Saarnio, S., and J. Silvola. 1999. Effects of increased CO<sub>2</sub> and N on CH<sub>4</sub> efflux from a boreal mire: a growth chamber experiment. *Oecologia* 119:349–356.
- Saarnio, S., S. Järviö, T. Saarinén, H. Vasander, and J. Silvola. 2003. Minor changes in vegetation and carbon gas balance in a boreal mire under a raised CO<sub>2</sub> or NH<sub>4</sub> NO<sub>3</sub> supply. *Ecosystems* 6:0046–0060.
- Saunois, M., et al. 2017. Variability and quasi-decadal changes in the methane budget over the period 2000–2012. *Atmospheric Chemistry and Physics* 17:11135–11161.
- Schaefer, K., T. Zhang, L. Bruhwiler, and A. P. Barrett. 2011. Amount and timing of permafrost carbon release in response to climate warming. *Tellus Series B* 63:165–180.
- Schimel, J. P. 1995. Plant transport and methane production as controls on methane flux from arctic wet meadow tundra. *Biogeochemistry* 28:183–200.
- Schulze, E. D., R. J. Scholes, J. R. Ehleringer, L. A. Hunt, J. Canadell, F. S. Chapin III and W. L. Steffen. 1999. Pages 19–44. The study of ecosystems in the context of global change. The terrestrial biosphere and global change—implications for natural and managed ecosystems. Cambridge University Press, Cambridge, UK.
- Schuur, E. A., et al. 2008. Vulnerability of permafrost carbon to climate change: Implications for the global carbon cycle. *BioScience* 58:701–714.
- Schuur, E. A. G., et al. 2015. Climate change and the permafrost carbon feedback. *Nature* 520:171–179.
- Sebacher, D. I., R. C. Harriss, and K. B. Bartlett. 1985. Methane emissions to the atmosphere through aquatic plants. *Journal of Environmental Quality* 14:40–46.
- Sellers, P. J., et al. 1997. BOREAS in 1997: Experiment overview, scientific results, and future directions. *Journal of Geophysical Research—Atmospheres* 102:28731–28769.
- Sharratt, B. S. 1992. Growing season trends in the Alaskan climate record. *Arctic* 45:124–127.
- Shaver, G. R., and F. S. Chapin. 1991. Production: biomass relationships and element cycling in contrasting arctic vegetation types. *Ecological Monographs* 61:1–31.
- Shaver, G. R., et al. 2000. Global Warming and Terrestrial Ecosystems: A Conceptual Framework for Analysis: Ecosystem responses to global warming will be complex and varied. Ecosystem warming experiments hold great potential for providing insights on ways terrestrial ecosystems will respond to upcoming decades of climate change. Documentation of initial conditions provides the context for understanding and predicting ecosystem responses. *BioScience* 50:871–882.
- Sitch, S., A. D. McGuire, J. Kimball, N. Gedney, J. Gamon, R. Engstrom, A. Wolf, Q. Zhuang, J. Clein, and K. C. McDonald. 2007. Assessing the carbon balance of circumpolar Arctic tundra using remote sensing and process modeling. *Ecological Applications* 17:213–234.
- Starr, G. E., S. F. Oberbauer, and E. R. I. C. W. Pop. 2000. Effects of lengthened growing season and soil warming on the phenology and physiology of *Polygonum bistorta*. *Global Change Biology* 6:357–369.
- Suyker, A. E., S. B. Verma, R. J. Clement, and D. P. Billesbach. 1996. Methane flux in a boreal fen: Season-long measurement by eddy correlation. *Journal of Geophysical Research* 101:28637–28647.
- Suyker, A. E., S. B. Verma, and T. J. Arkebauer. 1997. Season-long measurement of carbon dioxide exchange in a boreal fen. *Journal of Geophysical Research—Atmospheres* 102:29021–29028.
- Sweeney, C., et al. 2016. No significant increase in long-term CH<sub>4</sub> emissions on North Slope of Alaska despite significant increase in air temperature. *Geophysical Research Letters* 43:6604–6611.
- Tarnocai, C., J. G. Canadell, E. A. G. Schuur, P. Kuhry, G. Mazhitova, and S. Zimov. 2009. Soil organic carbon pools in the northern circumpolar permafrost region. *Global Biogeochemical Cycles* 23:GB2023, <https://doi.org/10.1029/2008GB003327>
- Thornton, B. F., M. Wik, and P. M. Crill. 2016. Double-counting challenges the accuracy of high-latitude methane inventories. *Geophysical Research Letters* 43:2016GL071772.
- Turetsky, M. R., C. C. Treat, M. P. Waldrop, J. M. Waddington, J. W. Harden, and A. D. McGuire. 2008. Short-term response of methane fluxes and methanogen activity to water table and soil warming manipulations in an Alaskan peatland. *Journal of Geophysical Research—Biogeosciences* 113:G00A10, <https://doi.org/10.1029/2007JG000496>
- Turetsky, M. R., E. S. Kane, J. W. Harden, R. D. Ottmar, K. L. Manies, E. Hoy, and E. S. Kasischke. 2011. Recent acceleration of biomass burning and carbon losses in Alaskan forests and peatlands. *Nature Geoscience* 4:27–31.
- Updegraff, K., S. D. Bridgman, J. Pastor, P. Weishampel, and C. Harth. 2001. Response of CO<sub>2</sub> and CH<sub>4</sub> emissions from peatlands to warming and water table manipulation. *Ecological Applications* 11:311–326.
- Wang, Z. P., R. D. Delaune, W. H. Patrick, and P. H. Masscheleyn. 1993. Soil redox and pH effects on methane production in a flooded rice soil. *Soil Science Society of America Journal* 57:382–385.
- Weinstock, B. 1969. Carbon monoxide: Residence time in the atmosphere. *Science* 166:224–225.
- Wendler, G., and M. Shulski. 2009. A century of climate change for Fairbanks, Alaska. *Arctic* 62:295–300.
- Whalen, S. C., and W. S. Reeburgh. 1988. A methane flux time series for tundra environments. *Global Biogeochemical Cycles* 2:399–409.
- Whalen, S. C., and W. S. Reeburgh. 1992. Interannual variations in tundra methane emission: A 4-year time series at fixed sites. *Global Biogeochemical Cycles* 6:139–159.
- Whiting, G. J., and J. P. Chanton. 1993. Primary production control of methane emission from wetlands. *Nature* 364:794.

- Winton, M. 2006. Amplified Arctic climate change: What does surface albedo feedback have to do with it? *Geophysical Research Letters* 33:L03701, <https://doi.org/10.1029/2005GL025244>
- Wylie, B., N. Pastick, K. D. Johnson, and H. Genet. 2016. Soil carbon and permafrost estimates and susceptibility in Alaska. in Z. Zhu and A. D. McGuire, editors. *Baseline and projected future carbon storage and greenhouse-gas fluxes in ecosystems of Alaska*. Professional Paper. U. S. Geological Survey, Reston, Virginia, USA.
- Yi, S., K. Manies, J. Harden, and A. D. McGuire. 2009. Characteristics of organic soil in black spruce forests: Implications for the application of land surface and ecosystem models in cold regions. *Geophysical Research Letters* 36:L05501, <https://doi.org/10.1029/2008GL037014>
- Yi, S., A. D. McGuire, E. Kasischke, J. Harden, K. Manies, M. Mack, and M. Turetsky. 2010. A dynamic organic soil biogeochemical model for simulating the effects of wildfire on soil environmental conditions and carbon dynamics of black spruce forests. *Journal of Geophysical Research: Biogeosciences* 115:G04015, <https://doi.org/10.1029/2010JG001302>
- Zehnder, A. J. B., and W. Stumm. 1988. Geochemistry and biogeochemistry of anaerobic habitats. Pages 1–38 in A. J. B. Zehnder, editor. *Biology of anaerobic microorganisms*. Wiley, New York, New York, USA.
- Zhu, Z., and A. D. McGuire, editors. 2016. *Baseline and projected future carbon storage and greenhouse-gas fluxes in ecosystems of Alaska*. U.S. Department of the Interior, U.S. Geological Survey, Reston, Virginia, USA.
- Zhuang, Q., A. D. McGuire, K. P. O'Neill, J. W. Harden, V. E. Romanovsky, and J. Yarie. 2002. Modeling soil thermal and carbon dynamics of a fire chronosequence in interior Alaska. *Journal of Geophysical Research: Atmospheres* 107(D1):8147.
- Zhuang, Q., et al. 2003. Carbon cycling in extratropical terrestrial ecosystems of the Northern Hemisphere during the 20th century: a modeling analysis of the influences of soil thermal dynamics. *Tellus Series B* 55:751–776.
- Zhuang, Q., J. M. Melillo, D. W. Kicklighter, R. G. Prinn, A. D. McGuire, P. A. Steudler, B. S. Felzer, and S. Hu. 2004. Methane fluxes between terrestrial ecosystems and the atmosphere at northern high latitudes during the past century: A retrospective analysis with a process-based biogeochemistry model. *Global Biogeochemical Cycles* 18:GB3010, <https://doi.org/10.1029/2004GB002239>
- Zhuang, Q., J. M. Melillo, M. C. Sarofim, D. W. Kicklighter, A. D. McGuire, B. S. Felzer, A. Sokolov, R. G. Prinn, P. A. Steudler, and S. Hu. 2006. CO<sub>2</sub> and CH<sub>4</sub> exchanges between land ecosystems and the atmosphere in northern high latitudes over the 21st century. *Geophysical Research Letters* 33:L17403, <https://doi.org/10.1029/2006GL026972>
- Zhuang, Q., J. M. Melillo, A. D. McGuire, D. W. Kicklighter, R. G. Prinn, P. A. Steudler, B. S. Felzer, and S. Hu. 2007. Net emissions of CH<sub>4</sub> and CO<sub>2</sub> in Alaska: Implications for the region's greenhouse gas budget. *Ecological Applications* 17:203–212.
- Zona, D., et al. 2016. Cold season emissions dominate the Arctic tundra methane budget. *Proceedings of the National Academy of Sciences USA* 113:40–45.

## SUPPORTING INFORMATION

Additional supporting information may be found online at: <http://onlinelibrary.wiley.com/doi/10.1002/eap.1755/full>

## DATA AVAILABILITY

Data available from the Scenario Network for Alaska Planning data portal: <https://doi.org/10.5066/t7td9w8z>